Li, Yaqi, Guan, Shaoliang, Huo, Hua, Ma, Yulin, Gao, Yunzhi, Zuo, Pengjian and Yin, Geping 2021. A review of magnesium aluminum chloride complex electrolytes for Mg batteries. Advanced Functional Materials 31 (24) , 2100650. 10.1002/adfm.202100650

Publishers page: http://dx.doi.org/10.1002/adfm.202100650

A Review of Magnesium Aluminum Chloride Complex Electrolytes for Mg Batteries

Yaqi Li[a], *Shaoliang Guan*[b,c], *Hua Huo* [a], *Yulin Ma* [a], *Yunzhi Gao* [a], *Pengjian Zuo**[, a], *Geping Yin***[,a]

a. MIIT Key Laboratory of Critical Materials Technology for New Energy Conversion and Storage, School of Chemistry and Chemical Engineering, Harbin Institute of Technology, Harbin 150001, China.

b. School of Chemistry, Cardiff University, Cardiff CF10 3AT, United Kingdom.

c. HarwellXPS, Research Complex at Harwell, Rutherford Appleton Laboratory, Didcot OX11 0FA, United Kingdom.

*Corresponding author.

E-mail: zuopj@hit.edu.cn

**Corresponding author.

E-mail: yingphit@hit.edu.cn

Abstract: Developing suitable electrolytes with high oxidation decomposition potential, low cost and good compatibility with electrode materials has been a critical challenge in realizing practical magnesium batteries. The emerging magnesium aluminum chloride complex (MACC) electrolytes based on inorganic chloride salts exhibit high Coulombic efficiencies and low overpotentials. This review summarizes recent studies of MACC electrolytes, focusing on the synthesis, characterization, and chemical environment of Mg species, electrolytic conditioning of electrolytes, and their application in typical magnesium batteries. The electrolyte evolution and influencing factor of electrolytic conditioning are discussed, and several kinds of conditioning-free MACC electrolytes are further introduced. Finally, future trends and perspectives in this field are discussed.

Key words: Magnesium aluminum chloride complex electrolytes, Mg batteries, electroactive Mg species, electrolytic conditioning, Al species, free Cl^- anions

1. Introduction

With the rapidly increase of demand for advanced energy storage, the constraints of lithium-based batteries in terms of safety, energy density, and cost have become very prominent. In recent years, non-lithium and multivalent metal ion batteries have attracted much attention [1]. Among them, magnesium battery as one of the alternatives shows great potential due to high reduction potential (-2.37 vs SHE), safety, and earth abundance in terms of Mg anode [2]. What's more, the specific volumetric capacity (3833 mA h cm^{-3}) of Mg is almost twice that of lithium metal (2046 mA h cm^{-3}) [3]. First prototype of the rechargeable Mg battery has been proposed by Aurbachs' group for about two decades [4]. However, there is still a long way for the Mg battery to be commercialized mainly due to the lack of feasible electrolytes [5]. The compatibility of electrolyte and electrode materials directly affects the working voltage and energy density of the battery. In fact, the development of electrolytes runs through the research of magnesium batteries. Generally, the Mg electrode is easily passivated in typical electrolytes consisting of simple Mg^{2+} salts (e.g. $MgCl_2$, $Mg(ClO_4)_2$, $MgSO_4$) and conventional polar solvents (e.g. ethylene carbonate, propylene carbonate, acetonitrile), leading to the irreversible Mg deposition [6]. In the early twentieth century, it was found that Grignard reagents can realize reversible Mg deposition [7], which laid the foundation for the development of Grignard-based electrolytes. However, the narrow electrochemical stability window of Grignard reagents limits their application in rechargeable Mg batteries. In 1990, it was found that adding strong Lewis acid $AlCl_3$ to Grignard reagent could enhance the anodic stability of electrolytes [6a]. Subsequently, the $Mg(AlCl_2R)_2$/tetrahydrofuran (THF) electrolyte and all-phenyl complex (APC) electrolyte were reported, enabling rechargeable magnesium batteries to be realized [4, 8]. However, the commercialization of Grignard-based electrolytes meets the challenge because of their nucleophilicity, high cost, and easy oxidation [9]. In fact, all organometallic components of alkali metals, alkaline earth metals, and aluminum are highly unstable in the environment of humid and air. In addition, the oxidative decomposition of organometallic usually limits the electrochemical window of Grignard-based electrolytes. The nucleophilic property of Grignard electrolytes makes it incompatible with electrophilic cathode materials such as sulfur. Therefore, it is necessary to develop non-nucleophilic and high anode stable electrolytes for Mg-S, Mg-O_2, and other high energy density Mg batteries [10].

Among non-Grignard based Mg battery electrolytes, the magnesium aluminum chloride complex (MACC) electrolytes have the characteristics of facile synthesis, low cost, high decomposition potential, enabling high Mg deposition/stripping Coulombic efficiency and low Mg deposition overpotential after electrolytic conditioning [11]. The MACC electrolytes can be obtained by the Lewis acid-base reaction of $MgCl_2$ and $AlCl_3$ in a variety of solvents such as THF, 1,2-dimethoxyethane (monoglyme, DME), which is similar to the synthesis of Grignard-based electrolytes[12]. Since MACC electrolyte was first proposed by Aurbach's group [9], much work on the composition, concentration, and electrolytic conditioning of MACC electrolytes has been carried out from experimental and theoretical aspects. However, as an emerging system, there are still many controversies and confusions regarding the understanding of MACC electrolytes. Regarding electrolyte synthesis and the effect of solvent and chlorides on electrolyte performance has not been systematically summarized, and in terms of the structure of magnesium complexes and electrochemically active species, it is inconclusive on the coordination number of the central Mg in MACC electrolyte. It remains in debate whether the dimeric or the monomeric Mg complexes are the dominant species responsible for Mg cycling. As for electrolytic conditioning, there is still no systematic understanding of impurity removal, optimization of magnesium complexes, changes in Cl^- existent form and so on, and it is also inconsistent whether the deposition of Al during electrolytic conditioning originates from cationic Al moieties or anionic $AlCl_4^-$.

This review on MACC electrolytes is arranged in the following sequences. In the first section, the synthesis of MACC electrolytes by different solvents and $AlCl_3/MgCl_2$ ratios are introduced. Next, the existent forms, characterization, and the role of Mg-Cl complexes and Al-Cl complexes in MACC electrolyte during cycling are discussed. Then, the active species, Mg/Al ratio, and impurities in the electrolyte during electrolytic conditioning are systematically summarized. Further, various factors affecting electrolytic conditioning are analyzed and various kinds of conditioning-free electrolytes are summarized. Finally, several electrochemical systems using MACC electrolytes are enumerated, and the existing problem and further trends of MACC electrolytes are also prospected.

2. Synthesis of MACC electrolytes

The MACC electrolyte is obtained by mixing a certain proportion of $MgCl_2$ and $AlCl_3$ in ether solvents. It is worth noting that different solvents, $MgCl_2/AlCl_3$ ratios can lead to different reaction mechanisms and require different synthesis notes. The purity of raw materials and the content of water and oxygen in the glove box also seriously affect the performance of the MACC electrolyte. Therefore, it can be understood that the electrolytes prepared in different groups or different batches are different. We try to find the unity of the synthesis method and the consistency of the reaction mechanism from different work.

2.1 The synthetic methods

The electrolyte of $MgCl_2$ in ether is difficult to realize the reversible deposition of Mg due to the low solubility of $MgCl_2$ [6, 9, 13]. The low solubility (about 7.8×10^{-4} M) of $MgCl_2$ in THF and endothermic reaction nature from $MgCl_2$ to $MgCl_2\cdot2THF$ indicate the insolubilization of $MgCl_2$ in the ether solvent [14]. The conductivity of $MgCl_2$ solution in ether is too low to be measured, leading to the irreversibility of Mg deposition [14]. However, the solubility of $MgCl_2$ can be increased by introducing Cl-containing Lewis acid. Barile et al. synthesized more than thirty solutions by mixing $MgCl_2$ with other chlorides including BCl_3, $AlCl_3$, $GaCl_3$ etc. in DME solvent [15]. It is found that the dissolution and deposition of Mg can be realized only in the electrolyte containing $MgCl_2$ with one of the five chlorides BCl_3, $AlCl_3$, $InCl_3$, $SnCl_2$, and $SbCl_3$. In addition, the anodic stability of $MgCl_2-MCl_x$ (M=B, Al, In, Sn, or Sb. X=2 or 3) electrolyte is closely related to the electronegativity of MCl_x, which can catalyze the decomposition of DME at high voltage. The more electronegative MCl_x is, the easier it is to extract electrons from the DME, leading to the decrease of anodic stability for the electrolyte. The oxidative decomposition potentials of $MgCl_2$-based solution with $InCl_3$, BCl_3, $SnCl_2$, or $SbCl_3$ are 2.0, 1.8, 1.5, and 1.2 V respectively, while that of $MgCl_2$-$AlCl_3$/DME is as high as 3.2 V. Therefore, the MACC electrolytes synthesized by the reaction of $AlCl_3$ and $MgCl_2$ in ether solvent shows great potential for secondary Mg batteries.

The solvents can affect the entropy changes during the electrolyte synthesis reaction, resulting in the different coordination numbers of the Mg-Cl complexes [15]. In most studies, the solvent for MACC electrolytes is THF or DME. As for the tetraethylene glycol dimethyl ether (G4, TEGDME, or TEG), some works believed that although the clear solution could be obtained due to the high solubility of the salts of MACC electrolytes in G4, the solution does not support effective Mg electrodeposition and dissolution due to strong chelation of solvent[15-16]. The chelation characteristics of long chain linear ethers inhibit the transfer of Mg^{2+} ions on the electrode surface[17]. The effect of $MgCl_2$/$AlCl_3$ ratios in G4 on electrolyte performance was further investigated[18]. It was found that the electrolytes with the $MgCl_2$: $AlCl_3$ ratios of 1:1, 1:2, and 1:3 showed higher ion conductivities and enabled reversible Mg cycling in comparison with the solution with $MgCl_2$: $AlCl_3$=2:1 ratio. It is speculated that the electrochemical activity of MACC/G4 electrolytes is strongly dependent on the $MgCl_2$: $AlCl_3$ ratio. In addition, some MACC electrolytes using mixed ether solvent including G4+1,3-dioxolane (DOL), G4+THF, or DOL+DME were reported for the reversible Mg deposition [16a].

The synthesis temperature affects the polymerization of solvent or solubility of electrolytes.

The process of $AlCl_3$ dissolved in THF is exothermic, which easily causes THF polymerization [19]. Electrospray ionization mass spectrometry (ESI-MS) studies showed that the as-prepared MACC electrolyte contains high molecular weight species with m/z values over 400, which are corresponding to oligomers of THF[20]. Similarly, the $AlCl_3$/THF solution also contains a large amount of polyTHF, indicating that the formation of polyTHF in MACC electrolytes is related to $AlCl_3$ [20]. In fact, the degree of THF ring-opening polymerization is related to the acidity of the Lewis acid [15]. Therefore, in the process of synthesizing MACC/THF electrolytes, $AlCl_3$ is generally added to THF slowly at 0 ℃ in order to avoid the formation of polyTHF which is detrimental to the electrochemical performance of MACC electrolytes. It is also reported that the MACC solution prepared at room temperature needs longer electrolytic conditioning cycling to eliminate the formed polyTHF.[20]. However, due to the low solubility of $MgCl_2$ at low temperatures, the electrolyte concentration is generally very low even with the addition of $AlCl_3$. In order to improve the concentration of the MACC electrolytes, the synthesis temperature can be raised to 30 or 45℃ when DME is used as solvent [21].

After a MACC electrolyte is prepared, the solutions consisting of $AlCl_3$ and $MgCl_2$ usually show high magnesium deposition/dissolution overpotential and poor reversibility. It was discovered that the electrochemical properties of the solution could be significantly improved by pre-electrochemical cycling, and the process is known as electrolytic conditioning[20]. The electrolytic conditioning is usually proceeding by a cyclic voltammetry process, which is normally conducted in a three-electrode system in which Pt as a working electrode and Mg foils as counter and reference electrode until a reasonable overpotential and Coulombic efficiency of magnesium deposition/dissolution are achieved.

2.2 Synthetic mechanism

It is worth noting that MACC electrolytes were developed from magnesium organohaloaluminate electrolytes which are usually prepared by Grignard type or MgR_2 type organometallic species and Al Lewis acid. However, the synthetic mechanisms of the two electrolytes are a little different. On one hand, the exchange of Mg-Cl and Al-Cl bond during the synthesis of MACC electrolytes is more difficult to occur thermodynamically, compared with the exchange of Mg-C and Al-C bond during the synthesis of magnesium organohaloaluminate electrolytes [15, 22]. On the other hand, the synthesis approach is termed as "mono-Cl abstraction", and the transmetalation reaction is realizing by only transferring Cl^- from $MgCl_2$ to $AlCl_3$ for MACC electrolytes; While for magnesium organohaloaluminate electrolytes, the ligand exchange reactions are more complex, and the undesired nucleophilic species MgR_2 is usually generated.

During the synthesis process of MACC electrolytes, $AlCl_3$ and $MgCl_2$ interact in the solvent to form new Al and Mg species. It was found that the Raman spectrum of $MgCl_2$/THF solution presented a large number of modes [23], indicating that the solution is heterogeneous caused by the poor solubility of $MgCl_2$ in THF. In contrast, the partial modes disappeared after the addition of $AlCl_3$ to $MgCl_2$/THF solution, indicating that the presence of $AlCl_3$ affects the type of Mg species. Meanwhile, the ^{35}Cl NMR spectra showed that the Mg-bound Cl in $MgCl_2+AlCl_3$/THF solution is deshielding compared with $MgCl_2$/THF solution, suggesting that the bound between Mg and Cl is tighter or the structure of Mg complexes has changed. The Raman spectra of the $AlCl_3$/THF solution showed only one obvious mode at 325 cm^{-1}, which is assigned to neutral $AlCl_3$ coordinated by THF [23]. After mixing $AlCl_3$/THF with $MgCl_2$/THF, the Al species changed from neutral $AlCl_3$ (325 cm^{-1}) to $AlCl_4^-$ anion (175 cm^{-1} and 211 cm^{-1}). The formation of ionic complexes should be the reason for the increased solubility of $MgCl_2$ [23].

The reaction products of electrolytes synthesis dependent on the ratio of $MgCl_2$ and $AlCl_3$ [24]. Taking MACC/DME electrolytes as an example, firstly, $MgCl_2$ is converted into $MgCl_2 \cdot 2DME$ with octahedral structure by DME solvent. Then one Cl^- in $MgCl_2 \cdot 2DME$ transfers to the chlorine-acceptor of $AlCl_3$, meanwhile the metastable $[MgCl \cdot 2DME]^+$ is formed. Next, In the case of the ratio of $MgCl_2$:$AlCl_3$=2:1, the monomer $[MgCl\cdot 2DME]^+$ polymerizes with a neutral $MgCl_2\cdot 2DME$ to form $[(\mu\text{-}Cl)_3Mg_2(\kappa^2\text{-}DME)_2(\kappa^1\text{-}DME)_2]AlCl_4$. In the case of the ratio of $MgCl_2$:$AlCl_3$=1:1, two monomers polymerize together and yield $[(\mu\text{-}Cl)_2Mg_2(\kappa^2\text{-}DME)_4](AlCl_4)_2$. In the case of $MgCl_2$:$AlCl_3$=1:2, a second Cl- abstraction of the monomer happens and the octahedron $[Mg(\kappa^2\text{-}DME)_3](AlCl_4)_2$ is produced finally **(Scheme 1)** [21].

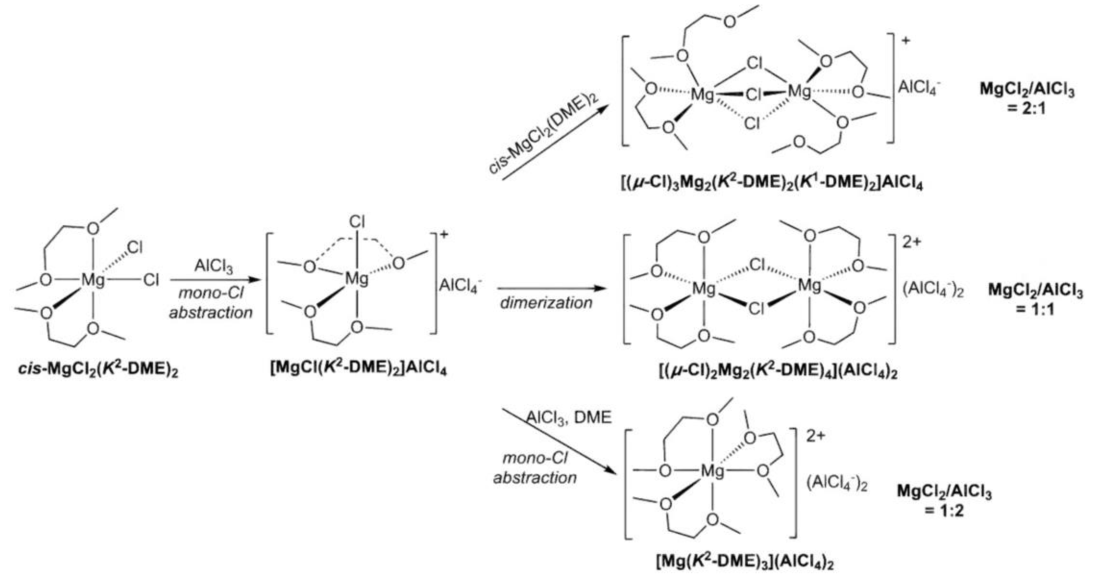

Scheme 1 Proposed reaction path of MACC electrolytes synthesis with various ratios of $MgCl_2$/$AlCl_3$. Reproduced with permission. [21] Copyright 2017, The Royal Society of Chemistry.

The synthetic of the MACC electrolytes in THF is similar to that in DME. When the ratio of $MgCl_2$ to $AlCl_3$ is 2:1, the $MgCl_2$ dissolves in THF to form $MgCl_2\cdot 3THF$. Then one part of $MgCl_2\cdot 3THF$ transforms into tetra-coordinated cation $[MgCl\cdot 3THF]^+$ which can further react with the other part of $MgCl_2\cdot 3THF$ to form $[(\mu\text{-}Cl)_3Mg_2\cdot 6THF]^+$. At last, there is an equilibrium between dimer $[(\mu\text{-}Cl)_3Mg_2\cdot 6THF]^+$, neutral $MgCl_2\cdot 4THF$, $MgCl_2\cdot 3THF$ and monomer $[MgCl\cdot 5THF]^+$ in the electrolyte [25]. The reaction equation is as following,

$$2MgCl_2+AlCl_3+6THF\rightarrow\left[(\mu\text{-}Cl)_3Mg_2\cdot 6THF\right]^+ +AlCl_4^- \quad (1)$$

In this section, the synthesis process of MACC electrolytes are introduced. The MACC electrolyte is obtained by mixing a certain proportion of $MgCl_2$ and $AlCl_3$ in ether solvent. It is worth noting that the electrolyte generally needs further electrolytic conditioning for use.

Moreover, various monomer and dimer magnesium complexes with different chemical environments are involved. During and after the synthesis, various Mg species are present at the same time and the major species depend on many factors such as solvent, $MgCl_2/AlCl_3$ ratio, and concentration. In the next section, we focus on the chemical environment, thermodynamic stability, and electrochemical activity of Mg species in MACC electrolytes.

3. The Mg species in MACC electrolytes

In the MACC electrolyte, there may be various forms of Mg species, such as monomer $[MgCl·3THF]^+$, dimer $[Mg_2Cl_3·2THF]^+$, $[Mg_2Cl_3·5THF]^+$, trimer $[Mg_3Cl_5·3THF]^+$, $[Mg_3Cl_5·4THF]^+$, etc. In the MACC electrolytes with different solvents, $MgCl_2$ and $AlCl_3$ ratios, the concentration and electrochemical activity of these Mg species may be different. Accurately detecting the Mg species including the coordination of Mg with Cl and solvent of the electrolyte before and after the electrolytic conditioning and during the electrochemical reaction is beneficial to guide the design of high-performance MACC electrolyte.

3.1 Detecting Methods for Mg species3.1.1 Single crystal X-ray diffraction (XRD)

In the study of magnesium electrolytes, the single crystal XRD is widely used to reveal the structure of Mg species [26]. By using this characterization, the Mg species in the 0.4 M MACC/DME electrolyte ($MgCl_2$: $AlCl_3$=2:1) is identified as $[Mg_2(\mu\text{-}Cl)_2(DME)_4][AlCl_4]_2$.[24] The cation complex consists of two octahedral coordinated Mg centers bridged by two chlorine atoms, and the four remaining sites of each Mg atom are coordinated through the oxygen atoms provided by two DME molecules, as shown in **Figure 1a**. However, the crystalline sample tested by single crystal XRD is usually obtained by the extraction and precipitation process from the electrolyte, and the detected Mg species are the most thermodynamically stable, which cannot fully reflect the actual chemical environment of the magnesium species in the liquid electrolyte [14].

3.1.2 Mass spectrometry (MS)

Electrospray ionization-mass spectrometry (ESI-MS) can analyze the charged species according to the mass-charge ratio (m/z), and the corresponding isotope pattern can directly detect the composition of electrolytes [27]. This direct detecting for electrolytes is very helpful to analyze the polymerization of solvent and distinguish monomeric and dimeric Mg species with various coordinated solvents. It is MS that first provided experimental evidence for the presence of $[MgCl\cdot 3THF]^+$ in an Mg-dimer electrolyte **(Figure 1b)** [28]. However, this characterization method also has some limitations. Firstly, the detected species may not only be in the electrolyte but may also be generated during the ionization process due to the damaging effect of the high-energy ionization source on the structure of the complex [11]. Although sub-ambient pressure ionization has a high-pressure process, and the dimer cation may lack sufficient stability under such test conditions. To solve this problem, Gewirth et al. reported [11] a soft ionization technology, the sonic spray ionization mass spectrometry (SSI-MS), to protect the dimer $[Mg_2Cl_3\cdot 6THF]^+$. However, there was still a problem that the solvent ligand was decomposed or dissolved in the ion chamber during the SSI process. With the soft ionization technology, the dimers $[Mg_2Cl_3\cdot 2THF]^+$ and $[Mg_2Cl_3\cdot 5THF]^+$ can be detected in the 0.06 M MACC/THF ($MgCl_2$: $AlCl_3$=2:1) electrolyte but the $[Mg_2(\mu\text{-}Cl)_3\cdot 6THF]^+$ still cannot be detected, possibly because some THF were weakly coordinated with Mg ions. Therefore, the second disadvantage of MS is that the binding of Mg-THF may be destroyed under the test conditions of ESI-MS due to excessively high temperatures [28]. In addition, it is difficult to test the high concentration electrolytes because the salts precipitate on the column and prevent the analyte from entering the spectrometer. Therefore, samples are often diluted before testing, and the change of electrolyte concentration will affect the equilibrium of Mg species [15], resulting in the inconsistency between the measured and the actual components of electrolytes.

3.1.3 Raman spectroscopy

Raman spectroscopy can also be used to detect the electrolyte directly and distinguish Mg dimer from Mg monomer. Raman spectra of $[Mg_2(\mu\text{-}Cl)_3\cdot 6THF]^+$ and $[MgCl\cdot 5THF]^+$ were simulated by Gewirth et al [11]. The structure of Mg species and the bond length of Mg-Cl and Mg-O bonds are confirmed from the density functional theory (DFT) calculation and single crystal XRD results. The Raman spectrum of dimer $[Mg_2(\mu\text{-}Cl)_3\cdot 6THF]^+$ appears the strongest peaks between 200 and 250 cm^{-1} and a shoulder in the slightly higher region; While the simulated Raman spectrum of the monomer complex $[MgCl\cdot 5THF]^+$ shows very little mode below 300 cm^{-1} **(Figure 1c)**.

3.1.4 Nuclear Magnetic Resonance Spectroscopy (NMR)

As a short-range technique for studying molecular structure and conformation, NMR is also an important method to detect the species of electrolytes [29]. The NMR parameters such as the isotropic chemical shift, quadrupolar parameters, scalar or dipolar coupling constants, and relaxation behavior can provide information about the local environment of the Mg and Cl nucleus. Generally speaking, the difference in charge density localization among Mg species in MACC electrolytes results in a unique NMR response of each nucleus [14]. The calculation results of the NMR shift for the Mg species in MACC electrolyte shows that the ^{35}Cl NMR spectrum can clearly distinguish monomer $[MgCl\cdot nTHF)]^+$ and dimer $[Mg_2Cl_3\cdot nTHF]^+$, while the ^{25}Mg NMR spectrum can be used to determine the number of coordinated THF **(Figure 1d)**.

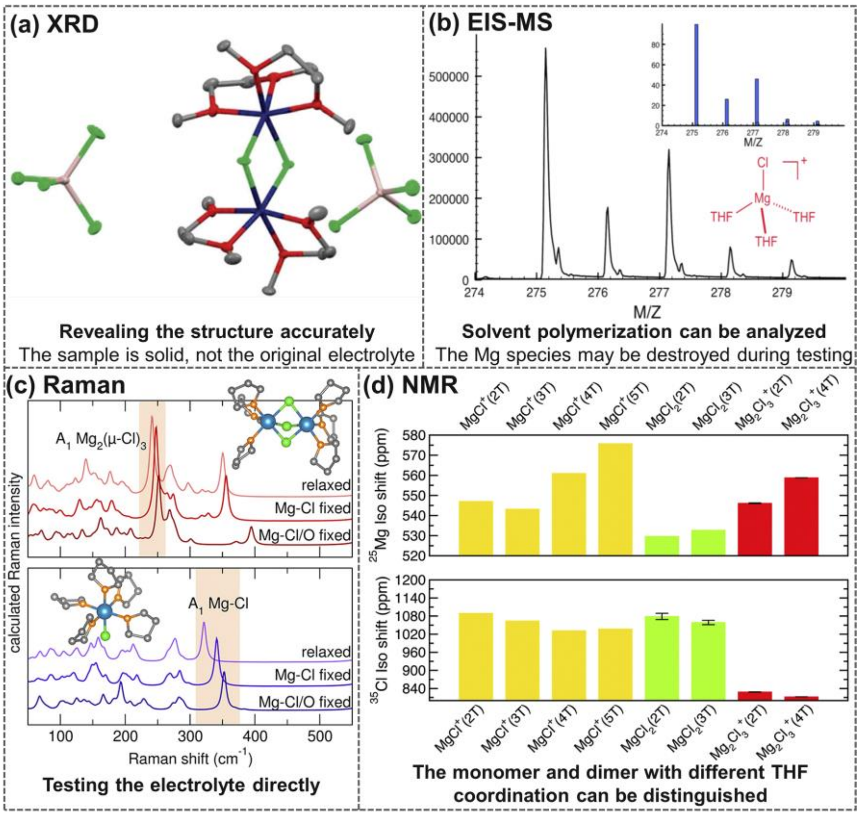

Figure 1. The characteristics and typical results of four methods for detecting Mg species. **a** Molecular structures of $[Mg_2(\mu\text{-}Cl)_2(DME)_4][AlCl_4]_2$. Reproduced with permission.[24] Copyright 2015, The Royal Society of Chemistry. **b** The m/z isotopic distribution of the $[MgCl(THF)_3]^+$ peak in the positive mode of SPIN MS of $[(\mu\text{-}Cl)_3Mg_2(THF)_6]AlPh_3Cl$. Reproduced with permission.[28] Copyright 2015, The Royal Society of Chemistry. **c** Calculated Raman spectra of $[Mg_2(\mu\text{-}Cl)_3\cdot 6THF]^+$ (the one above) and $[MgCl\cdot 5THF]^+$ (the one below) complexes. Reproduced with permission.[11] Copyright 2017, American Chemical Society. **d** ^{25}Mg and (the one above) ^{35}Cl NMR (the one below) spectra of magnesium-chloride complexes in the MACC electrolytes. Reproduced under the terms of the CC-BY 3.0 license.[14] Copyright 2015, The Royal Society of Chemistry.

3.2 Chemical environment of magnesium species in MACC electrolytes

The chemical environment of the Mg species includes two aspects, one is the coordination number of Mg^{2+}, and the other is the number of Mg central cations in the Mg species. In the non-aqueous electrolyte, the intercalation of magnesium ions usually requires the breaking of the Mg-Cl bond and the process of desolvation. Therefore, the chemical environment of the Mg central cation directly affects the deposition overpotential of Mg.

3.2.1 The coordination number of center Mg in Mg-Cl complexes

Due to the strong electrostatic interaction between Mg ions and the surroundings, Mg ions are usually coordinated by solvents or chloride ions in electrolytes. The oxygen in ethers solvent contains a lone pair of electrons that can coordinate with the empty orbitals of the magnesium center. It is meaningful to study the coordination of solvent to central cation, which will provide further understanding of the dependence of electrochemical deposition of magnesium on the solvent. Generally, Mg is considered as six-fold coordinated [12a, 25, 30], and it is also reported that the four-fold coordinated [14, 31] and five-fold coordinated [32] are stable. For magnesium organohaloaluminate electrolytes, six-fold coordinated Mg reported in some works was proved by the XRD results of the recrystallized electrolyte and the NMR and Mg K-edge X-ray absorption spectroscopy of solution [12b, 33]. The four-fold coordinated magnesium reported in other works was evidenced by near edge X-ray absorption fine structure (NEXAFS) spectra and Fourier processing extended X-ray absorption fine structure (EXAFS) spectra [31]. In the MACC electrolytes, it was found that there existed coordinated THF in $MgCl_2$/THF, $AlCl_3$/THF, and $MgCl_2$ + $AlCl_3$/THF solutions by comparing the Raman spectra of these solutions to pure THF [23]. The amount of coordinated THF around the Mg center in MACC electrolytes is limited by the bulkier structure of the ring. DFT calculations can be used to analyze the stability of magnesium-chloride clusters with different amounts of coordinated THF. It was reported that the magnesium species are the most stable when the coordination numbers of monomer, dimer, and trimer are 4, 5 and 6 respectively, and the corresponding stable magnesium species are $[MgCl\cdot 3THF]^+$, $MgCl_2\cdot 2THF$, $[Mg_2Cl_3\cdot 4THF]^+$ and $[Mg_3Cl_5\cdot 6THF]^+$ **(Figure 2a)** [14]. The classical molecular dynamics simulations (CMD) was further employed to study the coordination between THF and Mg ions. It was found that one part of THF molecules in the solvent is strongly coordinated with Mg ions, while another part is weakly coordinated with Mg ions, as shown in **Figure 2b** [14]. Thereby, the free exchange of THF in the first solvation layer with a large amount of THF in the bulk electrolyte can be realized. For example, for $Mg_2Cl_3^+$, two THF molecules strongly coordinate with each Mg ion, while the third THF molecule is constantly exchanged between the substantial electrolyte and the surroundings of Mg ions, resulting in 2.5 THF of effective coordination for each Mg ion. For the same reason, the effective coordination of THF with the Mg ion in monomer $MgCl^+$ is 3.7. The steric hindrance of THF and the charge transfer of Mg-Cl cause the Mg ion in MACC electrolytes failing to form the six-fold coordination which is commonly detected in solids. Wan et al. used First-principles molecular dynamics simulations (FPMD) to analyze the coordination of magnesium at room temperature, and similar results were obtained [32a]. It is found that the Mg centers in monomer tend to be four-fold coordinated in THF solution, and the stable structures are $MgCl_2 \cdot 2THF$ and $[MgCl \cdot 3THF]^+$, while six-fold coordination is unstable because of the high steric repulsion of THF. The stable structures of dimers are four-fold coordinated $Mg_2Cl_4 \cdot 4THF$ and five-fold coordinated $[Mg_2Cl_3 \cdot 4THF]^+$.

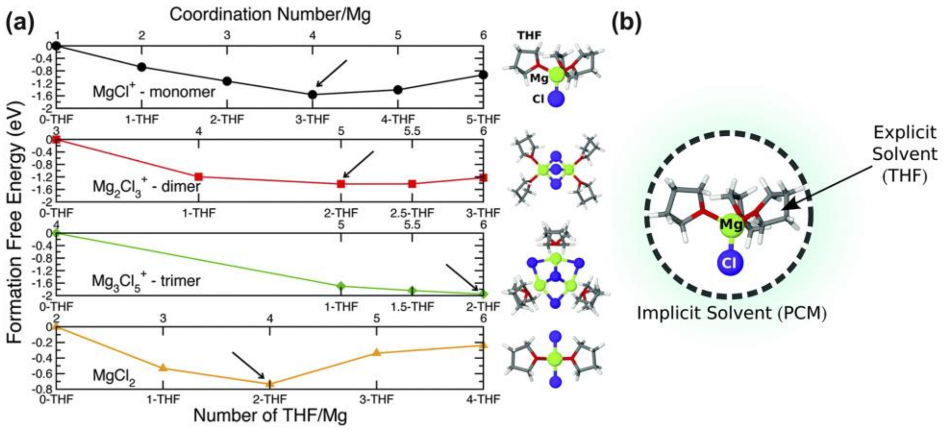

Figure 2. a Formation free energy of magnesium-chloride complexes as a function of THF coordination for magnesium-chloride complexes. **b** Diagram showing the approximation used to capture the solvation structure of magnesium-aluminum-chloride complexes. Reproduced under the terms of the CC-BY 3.0 license.[14] Copyright 2015, The Royal Society of Chemistry.

As mentioned above, because the magnesium species in the MACC electrolytes are mainly in the form of monomer or/and dimer (this issue will be summarized in the next section), the magnesium is four-fold coordinated and five-fold coordinated in most cases. The six-fold coordinated Mg is rare because trimer is not the main component of MACC electrolytes. The Mg ion in the solid phase is exactly hexa-coordinated, which has been proved by the simulation of X-ray absorption spectra (XAS) at the Mg K-edge and some other tests. In the process of detecting an electrolyte, if the dissolution/deposition kinetics of Mg is slow, the higher salt concentration may occur at the electrode/electrolyte interface, leading to the growth of oligomers or crystal-like precipitates at the interface. As a result, hexa-coordinated $[Mg_2Cl_3\cdot 6THF]^+$ will be generated on the surface of the magnesium electrode.

3.2.2 Monomer or dimer

Some viewpoints hold that the main Mg species in MACC electrolytes is dimer cation [23-24]. While some work thinks that monomeric Mg species is more dominant than dimer in the equilibrium of Mg species [28]. See et al. analyzed local atomic structure including the distance between the Mg center and the solvent molecules of the Mg species in the 0.06 M MACC/ THF ($MgCl_2$: $AlCl_3$=2:1) solution by pair distribution function (PDF), and found that the magnesium cation is in the form of octahedrally coordinated dimer $[Mg_2(\mu{-}Cl)_3\cdot 6THF]^+$ rather than tetrahedrally coordinated monomer [23]. Besides thermodynamic stability, the solubility of dimer magnesium is better than that of trimer and monomer no matter in THF [34] or in DME [21], which is beneficial to the standpoint that dimer is the dominating species in MACC electrolytes. While some work believes that under normal thermodynamic conditions, only $[MgCl\cdot 3THF]^+$ and $MgCl_2\cdot 2THF$ can exist steadily. Ceder et al. analyzed the stable phases of the Mg-Cl-Al-THF chemical space using the total energies of more than a hundred Mg_xCl_y and Al_xCl_y molecules with variable THF coordination numbers, and found that neither dimer nor trimer could exist in large quantities and stably in MACC/THF solutions [14]. The formation free energy of monomer ionic couples $[MgCl\cdot 3THF]^+AlCl_4^-$ and dimer $[Mg_2Cl_3\cdot 4THF]^+AlCl_4^-$ is 0.064 eV and 0.088 eV respectively, indicating that monomer is more likely to appear in MACC electrolytes [14]. However, under conditions of evaporating / drying solvent, dimers are more likely to appear. Some work also suggests that the monomer $[MgCl\cdot 3THF]^+$, dimer $[Mg_2Cl_3\cdot 2THF]^+$, $[Mg_2Cl_3\cdot 5THF]^+$, trimer $[Mg_3Cl_5\cdot 3THF]^+$, $[Mg_3Cl_5\cdot 4THF]^+$ and other magnesium species existed simultaneously in MACC electrolyte [11]. In general, monomer and dimer are common in most MACC electrolytes, but monomer is more difficult to detect.

3.3 Electrochemical active species during Mg deposition/dissolution in MACC electrolytes

Although both monomeric Mg complexes and multimers may exist in MACC electrolytes and maintain an equilibrium, not all Mg species can allow the reversible Mg deposition. It is still controversial on the electrochemical active species is monomer or dimer [3, 23]. Some work believes that during the Mg deposition process, most of species in the electrolyte are thermodynamically preferred Mg multimers. It is suggested that the Mg monomer is not conducive to electrochemical deposition in the 0.06 M MACC/THF ($MgCl_2$: $AlCl_3$=2:1) electrolyte, and the high overpotential of deposition is due to the effects of thermodynamically unfavorable monomeric Mg species in the early stage of electrolytic conditioning [20]. Barile et al. studied the electrochemical performance and the species of a series of $MgCl_2$-MCl_x (M=metal)/DME electrolytes, and found that the Mg deposition and stripping can occur only when electrolytes contain dimers and/or trimers, indicating that multimers were essential species for the electrochemical reaction [15]. Furthermore, all $MgCl_2$-MCl_x electrolytes containing Mg monomer require electrolytic conditioning to enhance the electrochemical activity of reversible magnesium deposition. While for the solution in the absence of Mg monomer, electrolytic conditioning is not necessary any more. The decrease of Mg monomer in the electrolytic conditioning process implies that Mg monomer inhibits the deposition and dissolution of Mg.

Some works hold the opposite view and believe that only monomer is electrochemically active. In terms of theoretical research, the formation energies of magnesium ions with Cl anions and THF molecules in monomers and dimers were calculated by DFT [32a]. It is found that when dimer cations are close to the electrolyte/electrode surface, the THF ligand is very difficult to remove, causing the large overpotential of Mg deposition. What's more, the coordination number to stabilize magnesium increases with the increasing number of Mg nuclei in Mg–Cl complex. The more coordination number, the more desolvation energy for magnesium deposition, meaning the more unfavorable magnesium deposition. In terms of experiment studies, there is no evidence that only Mg monomer is the active species in MACC electrolytes, but in electrolytes similar to the MACC, the mechanism of magnesium deposition/dissolution has been revealed in recent studies. Prakash et al. used X-ray absorption near-edge spectroscopy (XANES) spectroscopy to detect the species near the magnesium anode in the magnesium organohaloaluminate electrolyte and found that only the cationic monomer $[\mathrm{Mg}\ (\mu\text{-}\mathrm{Cl})\cdot 5\mathrm{THF}]^+$ can approach the Mg surface, rather than bulky dimers and trimers [33b]. Further, EXAFS was employed to analyze the Mg species during the deposition process of Mg, and it was found that there existed Mg intermediate on the Mg/electrolyte interface before Mg deposition [33b]. An equilibrium between monomers and dimers was proposed in magnesium organohaloaluminate electrolytes. During the deposition process of Mg, the monomer $[\mathrm{MgCl}\cdot 5\mathrm{THF}]^+$ adsorbs on the electrode firstly when a low potential is applied. Next, the monomer is reduced and dissociates on the electrode to form $[\mathrm{M}\text{-}\mathrm{Mg}]_{\mathrm{ads}}$ with the more negative potential. Finally, the adsorbed Mg^0 diffuses along the electrode surface to form $\mathrm{Mg}_{(\mathrm{m})}$ [33b]. Considering that the similar mechanism of Mg deposition and dissolution in the MACC and magnesium organohaloaluminate electrolyte [35], it is believed that Mg monomer also plays an important role in the deposition and dissolution of Mg in MACC electrolyte.

The significant function of monomeric Mg and the roles of dimeric Mg during Mg deposition were further revealed by studying the active species in $\mathrm{MgCl_2}$-Al Lewis acid electrolyte [28]. It is demonstrated that both monomer $[\mathrm{MgCl}\cdot 3\mathrm{THF}]^+$ and dimer $[(\mu\text{-}\mathrm{Cl})_3\mathrm{Mg}_2\cdot 6\mathrm{THF}]^+$ can participate in the first electron transfer reaction on magnesium anode, and the formed neutral $[\mathrm{MgCl}]^0$ adsorbs on the electrode surface. The formation of $[\mathrm{MgCl}]^0$ is the rate-determining step of magnesium deposition, and the metal magnesium forms from $[\mathrm{MgCl}]^0$ by the second electron transfer [28]. The viewpoint that both monomer and dimer are active species is also supported by the DFT calculations in Liu et al's work [36]. It is reported that the lowest unoccupied molecular orbital (LOMO) energy of $[(\mu\text{-Cl})_3Mg_2\cdot6THF]^+$ is a little higher than that of $[MgCl\cdot5THF]^+$, which means that the monomer is easier to be reduced. However, when subject to a one-electron reduction, the redox potential difference between two mono-cations is only 22 mV. Therefore, both $[(\mu\text{-Cl})_3Mg_2\cdot6THF]^+$ and $[MgCl\cdot5THF]^+$ mono-cations are almost equivalent for Mg deposition in terms of thermodynamics. They believe that both $[(\mu\text{-Cl})_3Mg_2\cdot6THF]^+$ and $[MgCl\cdot5THF]^+$ are electrochemically active, but dimeric Mg species is the main active species during magnesium deposition because dimer $[(\mu\text{-Cl})_3Mg_2\cdot6THF]^+$ is the main component in Mg-Cl complex electrolytes [36].

In this section, the Mg species in MACC electrolytes are highlighted, including the characterization method of the Mg species in the electrolyte, the chemical environment, and the change of the Mg species during the deposition and dissolution process. Three viewpoints on electrochemical active species in MACC electrolytes reported in previous literature are summarized. It is believed that the concentration of electrolyte, solvent, and $MgCl_2/AlCl_3$ ratio varies in different work, which affects the equilibrium of various Mg-Cl complexes and the electrochemical active species in the magnesium electrodeposition process. On the other hand, it is speculated that the current density, the type of magnesium deposition substrate, and the different stages of the magnesium electrodeposition process may correspond to different electrochemical active species. Understanding these issues is of great significance to the modification and improvement of the electrochemical activity of MACC electrolytes, which is worthy of making efforts in future work.

4. Electrolytic conditioning

Electrolytic conditioning is one of the most important features of MACC electrolytes. The tediousness of this process hinders the large-scale preparation of MACC electrolytes. Understanding the changes in the electrolyte during electrolytic conditioning is helpful to deduce the factors that affect the electrolytic conditioning period. Understanding the factors that affect the electrolytic conditioning period is the prerequisite for preparing the conditioning-free electrolyte.

4.1 MACC electrolyte evolution during electrolytic conditioning

As mentioned above, an electrolytic conditioning process is generally necessary for the freshly prepared MACC electrolytes. During electrolytic conditioning, the overpotential gradually decreases and the Coulombic efficiency gradually increases until the optimal magnesium deposition and dissolution property are achieved after a certain number of cycles **(Figure 3a and b)** [20]. Here we summarize four main changes of MACC electrolytes in the process of electrolytic conditioning.

4.1.1 The ratio of Mg to Al

Many studies have proved that there exists Al deposition during the electrolytic conditioning process of the MACC-like electrolyte with THF solvent [37]. For MACC/THF electrolytes, the Al deposition in the electrolytic conditioning process also was confirmed by a variety of methods. Firstly, the cyclic voltammetry (CV) curves of the 0.06 M MACC/THF ($MgCl_2$: $AlCl_3$=2:1) electrolyte in the first few cycles show that the current appears before the voltage reaches 0 V in the negative scanning process, which is corresponding to the deposition of Al (Figure 3a) [20]. Secondly, the scanning electron microscope (SEM) images were used to analyze the deposition products on Pt working electrode during different electrolytic conditioning stages for the 0.06 M MACC/THF ($MgCl_2$: $AlCl_3$=2:1) electrolyte [20]. It is found that the deposition is irregular before conditioning and there exists co-deposition of Al. With the proceeding of conditioning, the morphology of the deposition gradually becomes uniform, and the Al deposition gradually decreases and eventually disappears. Thirdly, Raman spectroscopy is also used to detect the changes of the 0.06 M MACC/THF ($MgCl_2$: $AlCl_3$=2:1) electrolyte before and after conditioning [23]. It is found that after electrolytic conditioning, the Mg−Cl associated stretches (~210 cm^{-1}) increase, and the strength of Al-Cl (~180 cm^{-1} and ~340 cm^{-1}) bond decreases **(Figure 3c)**, indicating that the concentration of Al-Cl complex decreases or the local coordination environment of Al changes. Fourthly, the XPS spectra of the Mg electrode show the Al signal increased after cycling the Mg/Mg symmetric cell with the 0.06 M MACC/THF ($MgCl_2$: $AlCl_3$=2:1) electrolyte 100 cycles, which is attributed to the irreversible deposition of Al [38]. In addition, the changes of intensity of ^{27}Al NMR spectrum and Al−Cl correlation confirmed by X-ray total scattering data also verify the decrease in concentration of Al species in the conditioned 0.06 M MACC/THF ($MgCl_2$: $AlCl_3$=2:1) electrolyte [23]. For the MACC/DME electrolytes, no Al deposition was observed during electrolyte conditioning in the 0.4 M MACC/DME ($MgCl_2$: $AlCl_3$=1:1) electrolyte [21]. The CV curves of the first few cycles in 0.06 M MACC/DME ($MgCl_2$: $AlCl_3$=2:1) show that there is no current appearing before the voltage reaches 0 V in the negative scanning process, indicating no deposition of Al **(Figure 3d)** [20]. However, See et al.'s work found a significant reduction in the Al species after conditioning in the 0.3 M MACC/DME ($MgCl_2$: $AlCl_3$=2:1) electrolyte by analyzing ^{27}Al NMR spectra [16a]. For MACC/TEG electrolytes, the Al deposition during electrolyte conditioning depends on whether the Al species in electrolytes contain $AlCl_2^+$ [18].

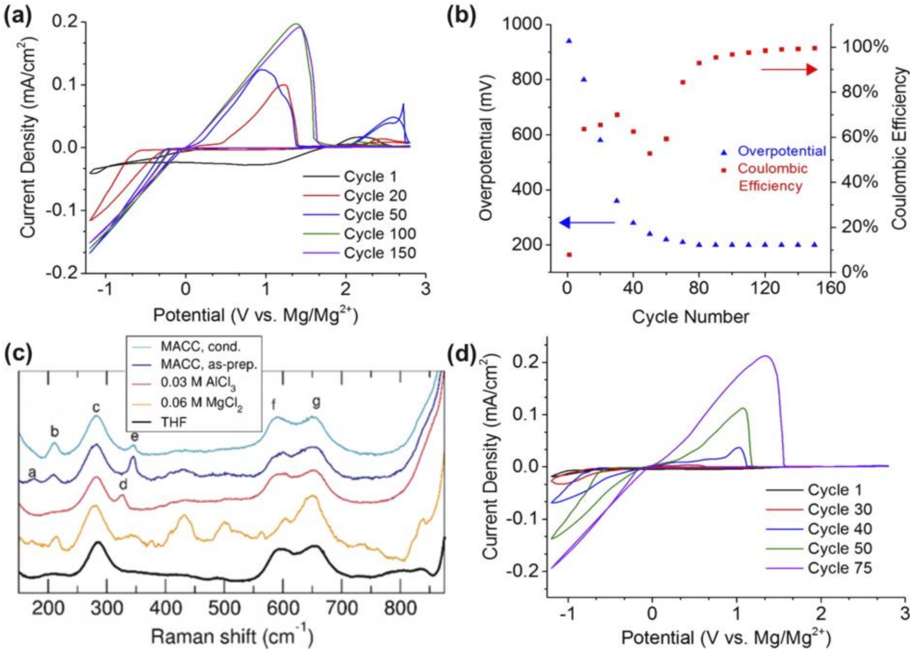

Figure 3. a CV curves of MACC/THF electrolyte at 5 mV/s on a Pt electrode. **b** Mg deposition overpotential and Coulombic efficiency of MACC/THF electrolyte as a function of cycle number. [20] **c** Raman spectra of the as-prepared and conditioned MACC electrolytes along with the component solutions. Reproduced with permission.[23] Copyright 2016, American Chemical Society. **d** CV curves of the MACC/DME electrolyte at 5 mV/s on a Pt electrode. a, b, d) Reproduced with permission.[20] Copyright 2014, American Chemical Society.

Accompanying with Al deposition, Mg oxidation occurs inevitably at the Mg counter electrode, leading to an increase of Mg concentration and Mg/Al ratio of conditioned MACC electrolytes. The improper ratio of Mg to Al can be regulated by electrolytic conditioning. Excessive addition of $MgCl_2$ or $AlCl_3$ to the conditioned 0.06 M MACC/THF ($MgCl_2$: $AlCl_3$=2:1) electrolyte would degrade the electrochemical performance of the electrolyte, and further cycling can restore the optimal deposition overpotential and Coulombic efficiency [20]. It was found the various initial Mg / Al ratios (1: 1 or 2: 1) of the as-prepared electrolyte can reach the same ratio of 2.6:1 after electrolytic conditioning, suggesting that the ratio of 2.6:1 seems to be the optimal ratio of Mg/Al in the conditioned electrolyte [20]. However, further research in the same work found that the fresh electrolyte with a Mg / Al ratio of about 2.6: 1 still could not achieve reversible deposition of magnesium in the first few cycles, indicating that the Mg/Al ratio of

2.6 was not a sufficient condition for MACC electrolytes to deliver good electrochemical performance. Therefore, the change of Mg/Al ratio is not the essential change in the electrolytic conditioning.

4.1.2 Types of Al-Cl complexes and Mg-Cl complexes

The equilibriums between Mg or Al species have important effects on the electrochemical performance, and the electrolytic conditioning can cause changes in these equilibriums. The reduction of the Al concentration in the electrolytic conditioning is beneficial to the conversion of Al-Cl complexes from electrochemical active to inert. ^{27}Al NMR spectrum can effectively distinguish the different Al species in the solution. It is confirmed that Al species in the 0.03 M $AlCl_3$/THF solution is mainly neutral $AlCl_3 \cdot 2THF$ as well as a small amount of $AlCl_4^-$and $[AlCl_2 \cdot 4THF]^+$. In the fresh 0.06 M MACC/THF ($MgCl_2$: $AlCl_3$=2:1) electrolyte, the Al-Cl complex is mainly $AlCl_4^-$ with a small amount of $[AlCl_2 \cdot 4THF]^+$ [23]. In the fresh 0.2 M MACC/TEG ($MgCl_2$: $AlCl_3$=1:2 or 1:3) electrolyte, the Al-Cl complexes are $AlCl_4^-$ anion in the majority with a small proportion of $AlCl_2^+$ [18]. At present, there is still a controversy about which Al species is electrochemical active and prone to deposition during electrolytic conditioning.

The one view believes that the deposition of Al comes from $AlCl_2^+$. The NMR spectrum of ^{27}Al shows that the Al species of the 0.2 M MACC in TEG ($MgCl_2$: $AlCl_3$=1:1) electrolyte contains only $AlCl_4^-$ **(Figure 4a)**, and no Al deposition can be observed during electrolytic conditioning. However, with the increase of $AlCl_3$ addition in the synthesis of MACC electrolyte, the formed $AlCl_2^+$ cations can cause Al deposition. After electrolytic conditioning, $AlCl_2^+$ decreases but the concentration of $AlCl_4^-$ remains unchanged **(Figure 4b and Fig 5b)** [18, 20]. It seems that that only $AlCl_2^+$ is involved in the aluminum deposition in conditioning. The reaction between 0.2 M MACC/TEG electrolyte with $MgCl_2$:$AlCl_3$=1:2 and Mg during electrolytic conditioning is as follows [18],

$$2AlCl_3 \leftrightarrow AlCl_2^+ + AlCl_4^- \quad (2)$$

$$AlCl_2^+ + 3e^- \leftrightarrow Al + 2Cl^- \quad (3)$$

$$Mg + Cl^- \leftrightarrow MgCl^+ + 2e^- \quad (4)$$

However, the aluminum deposition is not observed between the 0.2 M MACC/TEG electrolyte with $MgCl_2$:$AlCl_3$=1: 1 and Mg due to the lack of $AlCl_2^+$. In this case, $AlCl_2^+$ is converted to $AlCl_4^-$ by sufficient $MgCl_2$.

$$2MgCl_2 + AlCl_2^+ \rightarrow 2MgCl^+ + AlCl_4^- \quad (5)$$

The other view holds that $AlCl_4^-$ also has the electrochemical activity of Al deposition. In magnesium organohaloaluminate electrolytes, the Al species are usually in the form of AlR_4^-, AlR_3Cl^-, and $AlRCl_2^-$, and electrodeposition is not easy to occur due to the limitation of organic groups on deposition dynamics. However, in MACC electrolytes, the high proportion of Cl in $AlCl_4^-$ is the reason why Al is prone to electrodeposition. See et al. found that the peak area at 103 ppm in ^{27}Al NMR spectrum reduced due to the irreversible deposition of Al after plenty of cycles, suggesting that $AlCl_4^-$ was the main species that cause electrodeposition of Al during conditioning of the 0.3 M MACC ($MgCl_2$: $AlCl_3$=2:1) electrolyte[16a]. Gewirth et al found that besides the disappearance of the peak of $[AlCl_2 \cdot 4THF]^+$, the intensity of the ^{27}Al NMR signal corresponding to $AlCl_4^-$ decreased significantly and widened after electrolytic conditioning of the 0.06 M MACC/THF ($MgCl_2$: $AlCl_3$=2:1) electrolyte, indicating that $AlCl_4^-$ could also cause Al deposition **(Figure 4c)** [23]. It is generally believed that the reaction equation of Al electrodeposition caused by $AlCl_4^-$ in MACC/THF electrolytes is as follows [11, 23],

$$4AlCl_4^- + 6Mg + 6THF \rightarrow 4Al + 3\left[Mg_2(\mu\text{-}Cl_3)\cdot 6THF\right]^+ + 7Cl^- \quad (6)$$

In this review, we speculate that the electrodeposition may occur in both $AlCl_4^-$ and $AlCl_2^+$ during the electrolytic conditioning. However, different solvents have different chelating effects on central Al atoms, and the concentration and $MgCl_2$/$AlCl_3$ ratio of MACC electrolytes influence the content and ratio of the two Al species. Therefore, the priority and deposition conditions of the two Al species depend on the solvent, concentration, $MgCl_2/AlCl_3$ ratio, and other conditions.

As for the Mg-Cl complex, there was an increase of the low overpotential species after electrolytic conditioning **(Figure 5c)**. Electrolytic conditioning has an effect on the concentration of electroactive Mg species, which has been proved by X-ray Total Scattering results [23]. The pair distribution function (PDF) analysis was applied to reveal the bulk electrolyte composition in the mixed cation MACC system. The X-ray PDF provided detailed local structural information as a histogram of all atom-atom distances within MACC before and after conditioning, $AlCl_3$ solution, and $MgCl_2$ solution, which is helpful to identify changes in the local atomic structure as a result of conditioning. It shows that the intensity at 3.27 Å increases in the conditioned MACC compared to the as-prepared MACC **(Figure 4d)**, suggesting that there are more six-fold coordinated octahedral Mg species $[Mg_2(\mu\text{–}Cl)_3\cdot 6THF]^+$ in octahedral conditioned 0.06 M MACC/THF ($MgCl_2$: $AlCl_3$=2:1) electrolyte. It should be noted that the increase of the electroactive Mg species results from not only the increase of the total number of magnesium ions in the electrolyte, but also the change of equilibrium of the Mg complexes due to the increase of the Mg concentration **(Figure 4e)** [11].

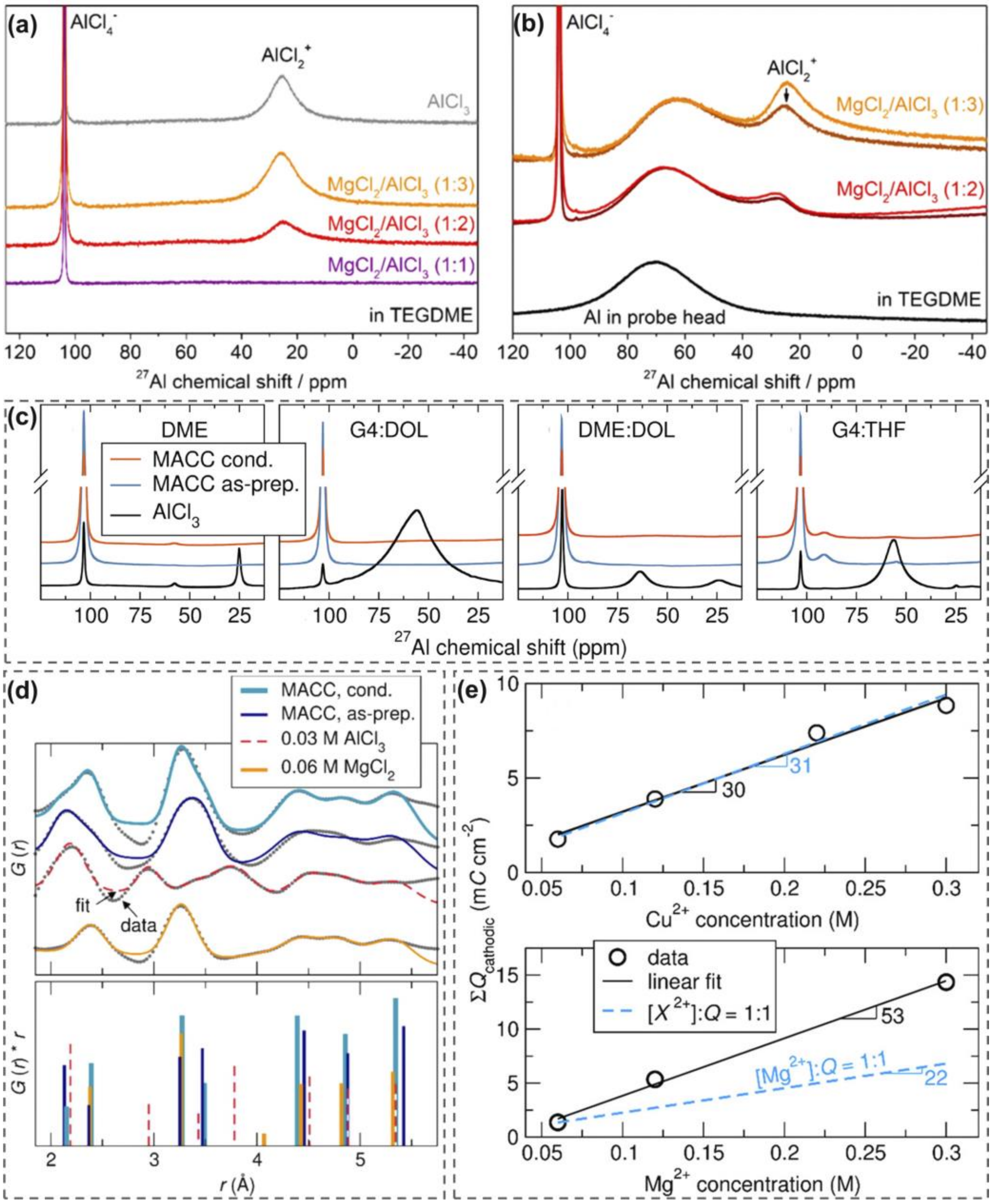

Figure 4. **a** ^{27}Al NMR of solutions of $AlCl_3$ and $MgCl_2/AlCl_3$ in ratios of 1:1, 1:2, and 1:3, based on the 0.2 M Mg salt in TEGDME. **b** ^{27}Al NMR spectra of $MgCl_2/AlCl_3$ (1:2) and (1:3) based on the 0.2 M Mg salt in TEGDME before and after 100 Mg dep./diss. cycles. a, b) Reproduced with permission. [18] Copyright 2019, American Chemical Society. **c** ^{27}Al NMR spectra of 0.15 M $AlCl_3$, as-prepared 5xMACC (0.3 M $MgCl_2$ and 0.15 M $AlCl_3$), and conditioned 5xMACC in DME, G4+DOL, DME+DOL, and G4+THF. The resonances are referenced to an internal coaxial $Al(NO_3)_3$ standard in D_2O (0 ppm). Reproduced with permission. [16a] Copyright 2019, American Chemical Society. **d** Fits of the XPDF data for the fresh MACC, conditioned MACC, and its component solutions. (i). Each component Gaussian is shown for all solutions to enable direct comparison. The magnitude of the bar chart corresponds to the area of each component Gaussian (ii). Reproduced with permission.[23] Copyright 2016, American Chemical Society. **e** Quantity of cathodic charge passed, $\Sigma Q_{cathodic}$, during electrodeposition of Cu^{2+} and Mg^{2+} as a function of the divalent ion concentration in the electrolyte. Reproduced with permission. [11] Copyright 2017, American Chemical Society.

4.1.3 The existent form of chloride ions

The Cl^- as the main ligand of the magnesium complex can not only activate Mg electrodes by dissolving surface oxides or removing adsorbed THF, but also act as an electron transfer bridge for Mg^{2+} during electrochemical reactions [30, 39]. In magnesium organohaloaluminate electrolytes, the "enhancement layer" containing Cl^- on Mg electrode can promote polycrystalline deposition and electron transfer at the electrode /solution interphase, facilitating the Mg deposition and dissolution [40]. In addition, Cl^- also can affect the deposition of magnesium by changing the equilibrium of magnesium species [12a, 28]. It was reported that the addition of a small amount of chloride ion can enhance the Mg deposition dissolution current density and the conductivity of $MgCl_2$–Al Lewis acid electrolytes [28].

Apart from the coordinated Cl^- which can act as ligand for central Mg or Al metal cation, the conditioned MACC electrolytes also contain free Cl^- anions. The existent form of Cl^- in MACC electrolyte changes and the amount of free Cl^- increases to facilitate the deposition/stripping of Mg during electrolytic conditioning. Surface enhanced Raman spectroscopy can effectively distinguish coordinated and free Cl^- anions in MACC electrolytes, although it is necessary to use Cu instead of Mg as a substrate due to the enhanced Cu−Cl stretches for characterization. It is reported that compared with the as-prepared electrolyte, the Cu-Cl stretch located at 300 cm^{-1} in the conditioned electrolyte is significantly enhanced, indicating that the concentration of free Cl^- in the electrolyte increases after conditioning [23]. Moreover, it could be also found that the aging MACC electrolyte showed inferior electrochemical activity due to the reduction of free Cl^- and adsorption of THF molecules on Mg. THF is a passivation component in the electrolyte and can spontaneously adsorb on the surface of Mg due to electrostatic interaction of Mg-O bond [32b]. The increasing free Cl^- during the electrolytic conditioning can reduce the adsorption of THF on Mg electrode further facilitate the deposition and stripping of Mg **(Figure 5d)**.

4.1.4 Impurities

Electrolytic conditioning can remove impurities such as water and polyTHF from the MACC electrolytes. In lithium batteries, trace-amount of H_2O (25–50 ppm) can be used as an electrolyte additive to solve the problem of lithium dendrite [41]. However, for electrolytes of magnesium batteries, even ppm level of water affects the active species and passivates Mg electrode, thus reducing the electrochemical activity of electrolytes. It is believed that the water and oxygen contents in glove box, the purity of as-received salts are important factors in determining Mg deposition/dissolution properties[42]. For Grignard-based magnesium organohaloaluminate electrolytes, trace water will affect the overpotential for Mg deposition by coordinating the Mg ions and retard the formation of the electroactive species for Mg deposition[43]. For the magnesium(II) bis(trifluoromethane sulfonyl)imide ($Mg(TFSI)_2$)/diglyme electrolyte, trace H_2O ($\leq$3 ppm) can suppress the reversibility of the Mg anode by forming a passivated film containing MgO and $Mg(OH)_2$ and slowing deposition kinetics due to the strong solvation of Mg^{2+} by water [39a]. In MACC electrolytes, the presence of water can hydrolyze $AlCl_3$ and $MgCl_2$ to form $Mg(OH)_2$ and $Al(OH)_3$, affecting the equilibrium among Mg-Cl complexes and reducing the concentration of Mg active species [38]. In addition, the newly deposited Mg quickly reacts with the water in electrolyte to form $Mg(OH)_2$, which can passivate the Mg electrode and eventually lead to the increased Mg deposition overpotential and low Coulombic efficiency. It was reported that the Coulombic efficiency of the 0.06 M MACC/THF ($MgCl_2$: $AlCl_3$=2:1) electrolyte prepared by undried $MgCl_2$ was 95%, which is significantly lower than that prepared by dried $MgCl_2$ (nearly 100%) [15]. When adding 20 ppm water to the 0.1 M MACC/DME ($MgCl_2$: $AlCl_3$=1:1) electrolyte, the overpotential of Mg deposition increased from 275 to 293 mV, and CE decreased from 87 to 84% [21].

During the electrolytic conditioning process, the deposition of Mg particles can consume the water in electrolyte, and the dry electrolyte with high electrochemical activity can be obtained [21]. Baltruschat's group used Differential electrochemical mass spectrometry (DEMS) to study the Mg deposition/dissolution process in the MACC electrolyte [16b]. Hydrogen could be obtained by the reaction between Mg and water in the electrolyte in the first few cycles, and it would gradually decrease during the following cycles [16b]. The change in the amount of hydrogen indicates that the water in the electrolyte gradually decreases with the electrolytic conditioning.

PolyTHF generated during the synthesis of MACC electrolytes is the other important impurity that deteriorates the dissolution/stripping of magnesium. As mentioned above in 4.13, the adsorption of THF on magnesium will passivate the electrode. Compared with THF, the interaction between polyTHF and the Mg surface is stronger, so the polyTHF is easier to adsorb on Mg and passivate the Mg electrode. What's more, it is suggested that the polyTHF affects the electrochemical activity of the electrolyte by changing the equilibrium of Mg species. Ceder et al believe that the amount of thermodynamically unfavorable monomer increases with the resting time because it is easily chelated by polyTHF [32b]. It is found that the addition of 5 wt % polyTHF to the MACC/THF electrolyte would increase the deposition overpotential of magnesium from ~ 200 mV to ~ 550 mV and reduce the Coulombic efficiency by 50 %. After electrolytic conditioning, the polyTHF in the MACC electrolyte disappeared according to the ESI-MS results [20]. However, if there are too many polyTHF in electrolytes, it is still difficult to support reversibly Mg deposition even after conditioning. For example, the polymerization of THF in $MgCl_2 + BCl_3$ / THF solution is so severe that it is not electrochemically active even after cyclic voltammetry for fifty cycles [15].

In addition, there are few studies on the influence of oxygen on the electrochemical performance and conditioning process of MACC electrolytes. It is reported that when the oxygen content in the MACC electrolyte is saturated, the reduction peak of oxygen rather than

Mg appears in the cyclic voltammetry curves [15]. However, it is not known whether the oxygen content in the electrolyte decreases with the electrolytic conditioning.

It should be noted that the removal of impurities is not the main factor in improving the performance of most conditioned electrolytes. If the removal of impurities is the main reason for Mg electrodeposition, the MACC electrolyte should maintain its activity over time. However, the MACC electrolytes generally suffer from aging problem, and the activity of Mg deposition/dissolution will decrease after about one week of resting for the conditioned electrolyte [23]. Moreover, if only the water and impurities in MACC electrolytes can be removed during the conditioning process the conditioning cycles should be related to the electrolyte concentration. However, it seems that the effect of electrolytic conditioning depends on the composition of as-prepared electrolytes. The inductively coupled plasma optical emission spectrometer (ICP-OES) results indicate that the conditioning the 0.2 M MACC/G4 electrolyte with a Mg/Al ratio of 1:1 mainly aimed to the impurity removal, while the conditioning of electrolyte with a Mg/Al ratio of 3:1 mainly aimed to the optimization of electrolyte composition [18].

According to the mentioned above, there are four main changes in electrolytic conditioning process of MACC electrolytes **(Figure 5a)**. Firstly, the concentration of magnesium ions increases, and the equilibrium between different Mg species moves towards the direction of increasing electrochemically active species, which is the most essential change of the electrolyte in electrolytic conditioning process; Secondly, the concentration of aluminum ions decreases, which is embodied in the electrodeposition of aluminum in the electrolytic conditioning and contributes to the formation of Mg species; Thirdly, the above changes are often accompanied by the conversion of coordinated Cl to free Cl, which helps to enhance the electrochemical activity of MACC electrolytes; Finally, the removal of impurities such as water and polyTHF is also an important modification during electrolytic conditioning. It is believed that this conclusion will help researchers to further study the factors influencing the electrolytic conditioning.

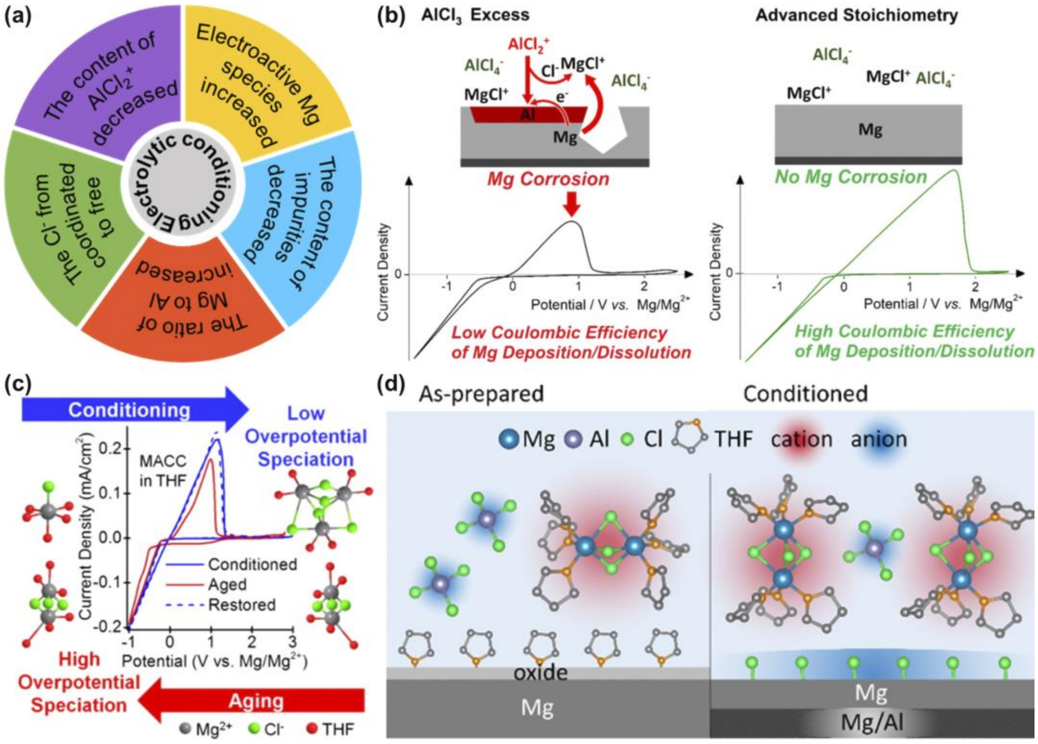

Figure 5. a The changes of MACC electrolytes in during electrolytic conditioning. **b** Schematic illustration of Al cementation/Mg corrosion in $AlCl_2^+$-containing electrolytes. Reproduced with permission.[18] Copyright 2019, American Chemical Society. **c** The CV curves and the changes of Mg species after conditioning. Reproduced with permission.[20] Copyright 2014, American Chemical Society. **d** Scheme depicting the speciation in as-prepared and conditioned MACC electrolyte solution. Reproduced with permission.[23] Copyright 2016, American Chemical Society.

4.2 Factors affecting the electrolytic conditioning and the performance of the conditioned MACC electrolytes

As summarized in the previous sections of Mg/Al ratio, the concentration and types of Al-Cl and Mg-Cl complexes, the impurity content can be optimized during electrolytic conditioning. Vice versa, the initial ratio of $MgCl_2$ to $AlCl_3$ during synthesis and impurity content in MACC electrolytes also affect conditioning period, although they are not the most substantial change during the electrolytic conditioning. Besides the two aspects, solvent, concentration, working temperature, and resting time have an important influence on conditioning period and the performance of conditioned electrolytes.

4.2.1 The solvent in the MACC electrolytes

The 0.06 M MACC/DME ($MgCl_2$: $AlCl_3$=2:1) electrolytes with various solvents were investigated during and after the electrolytic conditioning [15, 20]. The cyclic ether and chain ether solvents commonly used in MACC electrolytes are THF and DME, respectively. When THF is used as the solvent, the Coulombic efficiency was low at the beginning and increased to about 100% at about 50th cycles, and After conditioning, the onset of Mg deposition decreased to a constant value of ~200 mV [20]; When DME is used as a solvent, the Coulombic efficiency was increased to 92% and the overpotential for Mg deposition was ~150 mV after conditioning [20]; The 2-methyltetrahydrofuran (2-MeTHF) with larger steric and diglyme (G2) with longer chain are the other two ring ether and chain ether, respectively. When G2 is used as a solvent, the Coulombic efficiency of the electrolyte reached a steady value of ~94% and a little higher overpotential about 380 mV **(Figure 6a and b).** When 2-MeTHF was used as a solvent, the overpotential (about 350 mV) and Coulombic efficiency (about 80%) of magnesium deposition and stripping vary erratically after conditioning **(Figure 6c and d)** [15]; Both of the two solvents support Mg deposition/stripping, but the onset potentials for Mg deposition and the Coulombic efficiencies are inferior in comparison with those obtained in THF and DME. When 2,5-dimethyltetrahydrofuran (2,5-Me_2THF) and 2,2,5,5-tetramethyltetrahydrofuran (2,2,5,5-Me_4THF) with larger steric than 2-MeTHF were used as solvents, the electrolytes couldn't support Mg electrochemistry even after 75 cycles, suggesting that too much steric crowding around the O atom of ethers prevents the electroactive of Mg in MACC electrolyte. When triglyme (G3) and tetraglyme (G4) with longer chains than G2 are used as solvents, the electrolytes also fail to achieve disposition/striping of Mg after cycles, suggesting that the over-chelating properties also hinder the electroactivity of the Mg electrode.

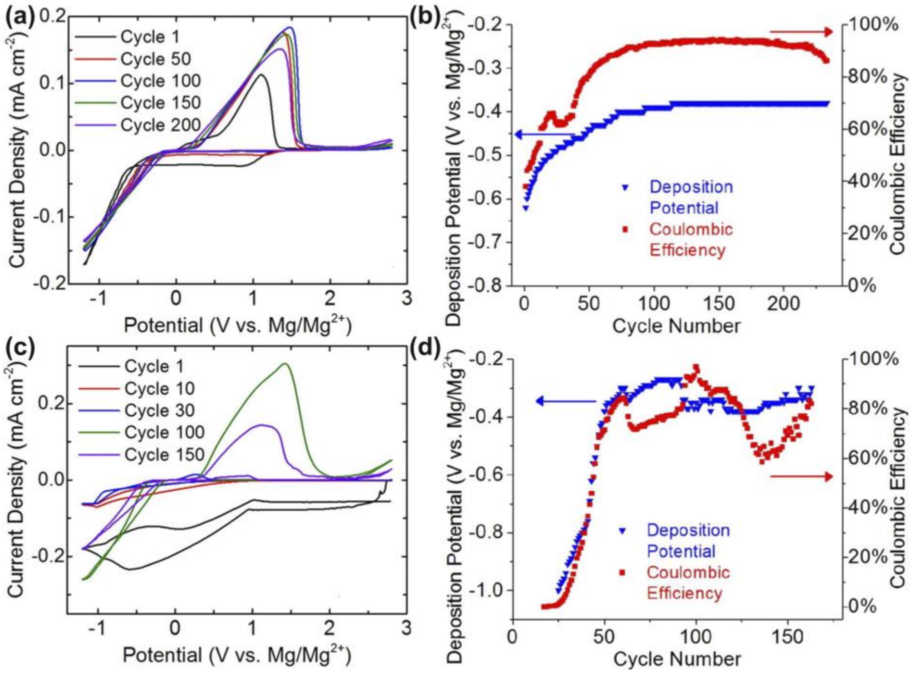

Figure 6. Cyclic voltammograms curves at different cycles of MACC electrolyte with various solvents at 5 mV/s on a Pt electrode. **a** diglyme; **c** 2-MeTHF; Mg deposition potential and coulombic efficiency as a function of cycle number of the MACC electrolyte in diglyme **b** and **d** 2-MeTHF. Reproduced with permission. [15].Copyright 2015, American Chemical Society.

The various properties of MACC electrolytes during and after the electrolytic conditioning may be due to various complexes in different solvents. Bevilacqua et al. characterized ^{27}Al NMR spectra of MACC electrolytes with four kinds of the solvent including DME, G4+DOL, DME+DOL, and G4+THF, and found that species in the $AlCl_3$ solutions varies with the solvent [16a]. In the MACC/DME electrolyte, besides the $AlCl_4^-$ which is located at 103 ppm, there is a resonance at 25 ppm assigned to $[AlCl_2{\cdot}4THF]^+$. While in the solutions with the other three solvents, the resonance of $[AlCl_2{\cdot}4THF]^+$ is not significant but the broad resonance at 64 ppm associated with neutral $AlCl_3$.2THF is obvious. And in the ^{27}Al NMR spectrum of electrolytes with G4+THF, there is a small resonance at 90 ppm assigned to some anionic complex, which is absence in the other three electrolytes.

4.2.2 The concentration of the MACC electrolytes

It is found that in MACC electrolytes, the peak of magnesium deposition and dissolution current density increased and the overpotential decreased significantly with the increasing concentration of electrolytes [21]. Furthermore, the higher concentration of electrolytes, the shorter conditioning period is. It is reported that the conditioning cycle numbers for 0.06 M, 0.12 M, and 0.3 M MACC electrolytes is 45, 35, and 18, respectively. After electrolytic conditioning, the overpotentials of the Mg deposition in the three electrolytes were 228 mV, 135 mV, and 59 mV, and the current densities at -0.5 V are -0.31 $mA\cdot cm^{-2}$, -1.5 $mA\cdot cm^{-2}$, and -4.3 $mA\cdot cm^{-2}$, respectively [11].

High concentration is beneficial to the rapid completion of electrolytic conditioning, which may be because the concentration of each component in the electrolyte does not change linearly with the increase of electrolyte concentration. For magnesium species, the electroactive Mg species increases faster than the electrolyte concentration due to the shift in the equilibrium of the Mg complexes [11], which we have described in Section 4.12. As for the influence of electrolytes concentration on equilibrium of Al species, the Al deposition in the electrolytic conditioning process of electrolytes with different concentrations has been studied [11]. The ^{27}Al NMR spectra show that the concentration of reduced $AlCl_4^-$ decreases with the increase of electrolyte concentration after conditioning, indicating that the amount of Al deposition in MACC electrolyte with high concentration is small. The ^{35}Cl NMR spectra show that few Al-Cl complexes converted into Mg-Cl complexes after the conditioning of high concentration electrolyte, indicating that there is relatively few Al deposition in the conditioning process of the high concentration electrolyte [11].

4.2.3 The working temperature of the MACC electrolytes

It is reported that MACC/THF electrolytes could complete the conditioning process quickly at a higher temperature, and the overpotential of magnesium deposition is lower and the Coulombic efficiency of Mg deposition/stripping is higher after conditioning [20]. From the kinetic point of view, the exchange rate between multimers and monomer is faster at higher temperatures, making the reversible magnesium deposition and dissolution easier. From the perspective of entropy (thermodynamics), the higher temperature is conducive to the conversion of the magnesium species to the monomer with the higher disorder. Considering that it is still controversial whether the electroactive species in MACC electrolytes are dimers or monomers, it is tentatively considered that the higher equilibrium conversion rate at higher temperature is the main factor to realize electrolytic conditioning.

4.2.4 The resting time of the MACC electrolytes

The MACC electrolytes have the issue of re-conditioning. The conditioned MACC electrolytes generally deliver poor magnesium deposition/stripping performance after resting for a few days. The aged electrolytes can recover the electroactivity again after applying CV scans again. The polymerization of THF during resting is the main challenge for the stability of MACC/THF electrolytes. ESI-MS spectrum shows that $[(THF)_{13}\text{-}C_2H_4 + H]^+$ is generated after resting the conditioning of MACC/THF electrolyte for one week, and can be removed after re-conditioning [20]. The problem of undesirable oligomers generated after resting mainly exists in MACC electrolytes with THF solvent. While the performance degradation of MACC electrolytes with chain ethers (such as DME) is not so severe after resting. ESI-MS spectra prove that there were no oligomers produced in the as-prepared, conditioned, and rested MACC/DME electrolytes [20]. In addition to THF polymerization, it is believed that the decrease in the amount of free Cl^- is also an important reason for the aging of MACC electrolytes [20, 23]. The third reason for the aging of MACC electrolytes is that some active species in the MACC/THF electrolyte reacts with Mg to produce Al and neutral $MgCl_2 \cdot 2THF$ when exposing the electrolyte to Mg according to the following reaction equation [14].

$$AlCl_4^-(l) + MgCl^+(3THF)(l) + 1.5\ Mg(s) + 2THF(l) \rightarrow 2.5\ MgCl_2(2THF)(l) + Al(s) \tag{6}$$

It is worth noting that some works believe that the reaction between Mg metal and MACC electrolytes with various solvents including THF, DME, G2, and G4 is beneficial to increase the electrochemical activity of the electrolyte in the absence of applied voltage [18, 44]. This reaction consumes the unexpected $AlCl_2^+$ in electrolytes [18]. Therefore, whether the contact between MACC electrolytes and magnesium during storage will cause the aging of the electrolyte may be related to the existent form of Al species and the corresponding reactivity of Al species in solutions with different chemical environments.

In summary, factors such as initial $MgCl_2$ / $AlCl_3$ ratio, impurity content, solvent, temperature, and electrolyte concentration affect the conditioning period and electrochemical performance of MACC electrolytes by influencing the chemical environment, coordination structure, concentration, and migration rate of electroactive species in MACC electrolytes. Understanding the factors and mechanisms that affect electrolytic conditioning is conducive to the development of conditioning-free MACC electrolytes.

4.3 Conditioning-free MACC electrolytes

Methods such as reducing impurities content, increasing the concentration of raw materials, and reasonable temperature control are beneficial to reduce the conditioning period of the electrolyte. At present, the literature mainly adopt the following ideas to prepare the conditioning-free electrolytes.

4.3.1 Adding magnesium salt additive to MACC electrolytes

There are three main functions of Mg salt additive. Firstly, removing impurities. It is reported that the addition of MgH_2 can effectively remove the 53 ppm water in the 0.5 M MACC/TEG ($MgCl_2$:$AlCl_3$ =1:1) electrolyte [16b]. The Bu_2Mg is conducive to remove impurities and improve the electrodeposition performance of electrolytes for Mg batteries [18, 45]. After adding a small amount of Bu_2Mg (10 mM) in the 0.2 M MACC/TEG ($MgCl_2$:$AlCl_3$ =1:1) electrolyte, the Mg deposition/stripping at low overpotentials and shows high Coulombic efficiency at the first cycle [18]. $Mg(TFSI)_2$ as another Mg salt can improve the water resistance of the as-prepared

MACC/THF electrolyte [38]. The Coulombic efficiency of Mg for the Mg(TFSI)$_2$ modified 0.06 M MACC/TEG ($MgCl_2$:$AlCl_3$ =2:1) electrolyte is as high as 97%, and the overpotential for magnesium deposition is as low as 0.10 V. Moreover, it remains active even after the introduction of 2000 ppm of water or when prepared from undried raw materials. Magnesium hexamethyldisilizide (HMDS, $N[Si(CH_3)_3]_2^-$) is also a strong water scavenger [46]. The HMDS$^-$ can react with water to form OH^- and HMDS. Karl Fischer titration testing shows the water content of the 0.06 M MACC/THF ($MgCl_2$:$AlCl_3$ =2:1) electrolyte with 2 mM Mg(HMDS)$_2$ additive is 46 ppm, which is 25 ppm lower than that of the electrolyte without Mg(HMDS)$_2$. In addition, it has been reported that trace amounts of $Mg[BH_4]_2$ also can be used to remove H_2O and enhance reversible Mg electrochemistry [47], but it has not been applied in MACC electrolytes. Secondly, magnesium salt additives can enhance the electrochemical activity of the electrolyte by changing the equilibrium of magnesium species in MACC electrolytes. The strategy of dual magnesium salt has been widely used in magnesium battery electrolytes [48]. In Xu et al.'s work, the addition of Mg(TFSI)$_2$ not only removes water impurities in the MACC electrolyte, but more importantly, it also increases the concentration of active Mg species [38]. By the analysis of single crystal XRD, there is extra $[Mg_2(\mu\text{-}Cl)_3\cdot 6THF]^+\cdot[TFSI]^-$ existing in the electrolyte besides $[Mg_2(\mu\text{-}Cl)_3\cdot 6THF)]^+\cdot[AlCl_4]^-$ after the addition of Mg(TFSI)$_2$. It is suggested that the increase in $[Mg_2(\mu\text{-}Cl)_3\cdot 6THF]^+$ is the main reason for facilitating the electro-deposition. Thirdly, the addition of magnesium salt also affects other components in electrolytes, such as $AlCl_4^-$ and free Cl^-. For example, Mg(HMDS)$_2$ additive can react with $AlCl_4^-$, resulting in a decrease in the amount of $AlCl_4^-$ and an increase in free Cl^- which can be modified on the surface of the Mg electrode to facilitate the electrodeposition of Mg [46]. By adding a small amount of Mg(HMDS)$_2$ to the MACC electrolyte, Al deposition can be inhibited and reversible Mg electrodeposition and stripping can be achieved in the first cycle **(Figure 7b)**. However, this electrolyte still has the problem of aging because of the instability of free Cl^- anions.

4.3.2 Adding Mg powders during the synthesis of MACC electrolytes

Adding magnesium powders to MACC electrolytes is another important method to prepare the conditioning-free electrolytes. In terms of the reasons why conditioning-free MACC electrolytes can be realized, the introduction of Mg powder in the synthesis of electrolytes is similar to the addition of magnesium salt additives in electrolytes. Firstly, some Al species in electrolytes can be reduced by Mg powder, which avoids the co-deposition of Al. The second one is that the free Cl^- can replace the solvent adsorption on the electrode surface and avoid passivation during the reaction between Mg powder and aluminum species. In addition, the reduced Mg powder can be used as a scavenger to remove the impurities such as H_2O in MACC electrolytes. Luo et al.'s work indicates that after adding 50 ppm water to MACC electrolyte, the overpotential increased to 350 mV and the Coulombic efficiency decreased to 86%. After adding Mg powder, the electrochemistry performance of the MACC electrolyte with 50 ppm water was restored [44]. The Mg powder also has the function of removing some Al species which usually causes co-deposit during electrolytic conditioning of MACC electrolyte. Mg powder can react with some Al species, which is confirmed by the fact that the $AlCl_3$/THF solution of Mg powder can realize slight Mg deposition/stripping after resting for 20 hours [44]. Based on the active role of magnesium powder in electrolyte synthesis, Luo et al. reported an electrolyte synthesized by mixing Mg powder, $MgCl_2$ and $AlCl_3$ in THF, and they named it MMAC electrolyte **(Figure 7c)**. The Mg deposition overpotential of the MMAC/THF electrolyte (159 mV) was even lower than that of the conditioned MACC electrolyte (165 mV). The inductively coupled plasma mass spectrometry (ICP-MS) results showed that the Mg/Al ratio of MACC electrolyte with THF, DME, and G2 solvent increased from 2:1, 1:1, 1:2 to 2.39:1, 1.45:1, 1:1.22 respectively when the magnesium powder was involved in electrolyte synthesis [44].

4.3.3 Replacing $MgCl_2$ with metallic magnesium as the magnesium ion source to synthesize MACC electrolytes

In addition to using magnesium powder as an auxiliary reactant, some work also uses Mg powder directly as a source of magnesium ions to synthesize MACC electrolytes. Ha et al. reported a method using $CrCl_3$ as the "initiator" for the reaction between $AlCl_3$ / THF and Mg metal to generate a magnesium aluminum chloride complex electrolyte. The electrolyte shares many characteristics with traditional MACC electrolyte, but can achieve 100% magnesium deposition and dissolution Coulombic efficiency in the first cycle. The advantage of conditioning-free is due to the extremely high Mg/Al ratio in the electrolyte [49]. Recently, Li et al. [50] also proposed a conditioning-free MACC like electrolyte (denoted as MAT electrolyte) which was synthesized by mixing Mg powders, $AlCl_3$ and $TiCl_4$ in TEG solvent. It is worth noting that although the raw materials used in these two synthesis methods are similar, the synthetic mechanism and composition of electrolytes are different. In the former work, the magnesium species in the electrolyte is dimeric $[Mg_2Cl_3 \cdot 6THF]^+$ and the concentration of magnesium ions is about 0.28 M. For the electrolyte synthesis, the Cr_pAl_q and $MgCl_2$ form firstly, and the $MgCl_2$ reacts with $AlCl_3$ to generate $[Mg_2Cl_3 \cdot 6THF]^+$ and $AlCl_4^-$. At last, the $AlCl_4^-$ further reacts with the Cr_pAl_q-covered Mg in solution to generate $[Mg_2Cl_3 \cdot 6THF]^+$ and Al. In the latter work, the magnesium species in the electrolyte with the magnesium ion concentration of 0.73 M is monomeric $[MgCl \cdot TEG]^+$ and $[MgCl \cdot 2TEG]^+$. For the MAT electrolyte synthesis, it can be found that the $AlCl_4^-$ is originally present in $AlCl_3$/TEG solution and could not react with Mg directly. Moreover, although Ti cluster can facilitate the adsorption of Al atoms on the Ti cluster-modified Mg(0001) **(Figure 7d)**, Ti-modified Mg foil still cannot react with $AlCl_4^-$ effectively. The intermediate product $Al_2Cl_7^-$ produced during electrolyte synthesis is the necessary species for Al deposition. The difference in the synthetic mechanism between these two works may be caused by the chemical environments of the Mg-Cl complex and the Al-Cl complex in different solvents, and different initiators may also cause different reactivity of magnesium.

Therefore, removing impurities, increasing the concentration of active species and the amount of free Cl^- are important ideas for the development of conditioning-free electrolytes. Based on these considerations, adding Mg powder and Mg salt and changing the source of magnesium ions are effective strategies **(Figure 7a)**. For traditional MACC electrolytes, many CV cycles are required to achieve good reversibility of a small amount of conditioned electrolytes. The tedious electrochemical conditioning process makes it difficult to produce high performance MACC electrolytes on a large scale. So, the discovery of conditioning-free electrolytes is a major breakthrough in the development of MACC electrolytes, which is helpful to the application of MACC electrolytes in full batteries.

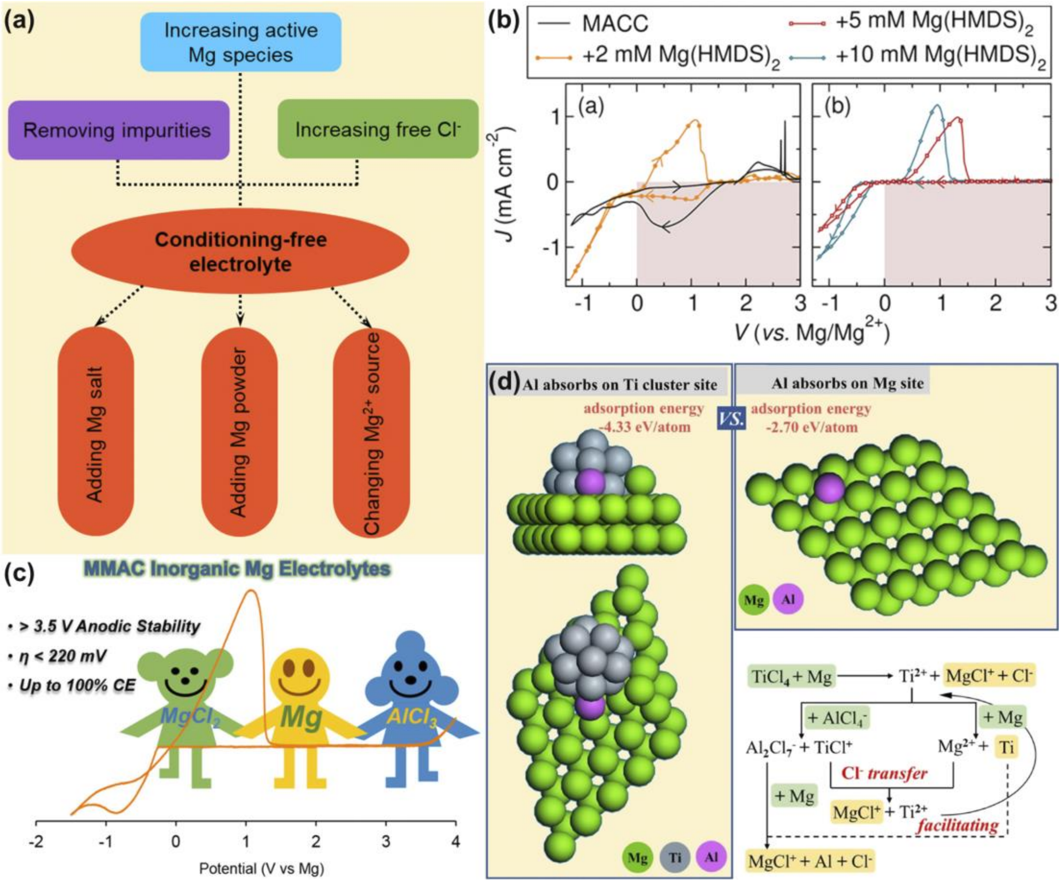

Figure 7. a The mind mapping of conditioning-free MACC electrolyte. **b** First CV cycles of MACC and MACC+2 mM $Mg(HMDS)_2$, MACC+5 mM $Mg(HMDS)_2$, and MACC+10 mM $Mg(HMDS)_2$ electrolytes. Reproduced with permission.[46] Copyright 2020, American

Chemical Society. **c** The CV curve of MACC electrolyte prepared from $MgCl_2$, $AlCl_3$ and Mg powder. Reproduced with permission.[44] Copyright 2017, American Chemical Society. **d** Proposed reaction sequences in the formation of MAT electrolyte (The solvation is omitted). Reproduced with permission. [50] Copyright 2021, Elsevier.

5. Application of MACC electrolytes in full batteries

At present, the development of MACC electrolyte is still in the preliminary stage, and there are few reports on its application in full battery in the published literature. Some promising cathode materials, such as MOFs, SnS_x, and WSe_2, have not yet been used in magnesium ion batteries based on MACC electrolytes.[51] Regarding the modified interface between anode and electrolyte, some effective schemes have been proposed in the aqueous electrolyte[52] and other organic electrolytes[53], but there is a lack of relevant reports in the magnesium ion battery with MACC electrolyte. In addition, there is still a lack of effective methods to solve the corrosion problem of Cl^- in MACC electrolyte to metal subassembly and collector. Herein, we select several typical battery systems with MACC electrolytes, which are magnesium ion batteries matched with insertion type cathode material, magnesium sulfur battery matched with conversion type cathode material and hybrid battery matched with lithium-ion battery cathode material.

5.1 Application of MACC electrolytes in magnesium ion batteries

The Mo_6S_8 with Chevrel phase is often used as a cathode material for magnesium ion batteries [54]. In MACC electrolyte, the active Mg species are $MgCl^+$ and $Mg_2Cl_3^+$. During the insertion of Mg ions, the strong ionic Mg-Cl bond is broken, and then Mg ion is inserted into the Chevrel phase while the remaining Cl^- ions can be combined with Mo in Mo_6S_8. The chlorinated surface can promote the further insertion reaction by interacting with the $MgCl^+$ near the cathode [55]. In the organic MACC electrolyte system, the insertion of Mg^{2+} into the cathode material needs complete desolvation. However, Mg^{2+} can undergo partial dehydration in aqueous electrolyte, which promotes the interaction of Mg^{2+} with the framework constituents and fast diffusion of

Mg^{2+} [56].Doe et al.[9] applied the MACC electrolyte in the Mo_6S_8/Mg battery, and the discharge voltage platform of about 1.1 V is comparable to the cell with Grignard-based electrolyte. The only drawback is that the discharge specific capacity of the first eight cycles at 1/15 C is about 80 mAh·g^{-1}, which is far lower than the theoretical specific capacity (128 mA h·g^{-1}) of Mo_6S_8. In 2016, Ha et al. applied the conditioning-free MACC electrolyte in Mo_6S_8/Mg battery, and the battery delivered the satisfying discharge specific capacities of 110 mAh·g^{-1} at 1/8 C and 80 mA h g^{-1} at 1 C for 250 cycles **(Figure 8a)** [49]. The other conditioning-free electrolyte MACC-$Mg(TFSI)_2$ was also used in the Mo_6S_8/Mg battery, and the batteries exhibited better discharge specific capacity and cyclic stability compared with the ones with the organoaluminate-based electrolyte and $Mg(BH_4)_2$-$LiBH_4$/G2 electrolyte [38]. These outstanding works lay the foundation for the further development of MACC electrolytes in magnesium ion batteries.

5.2 Application of MACC electrolytes in magnesium-sulfur batteries

As a high capacity (1675 mA h g^{-1}) cathode material, sulfur has attracted many attentions in metal-sulfur systems such as lithium-sulfur [57], sodium-sulfur [58], potassium-sulfur [59], aluminum-sulfur [60], calcium-sulfur [61], and magnesium-sulfur [62] batteries. The theoretical discharge platform of Mg-S batteries is as high as 1.77 V, and the charging cut-off potential of magnesium sulfur batteries [63] is usually higher than that of magnesium ion batteries with the cathode materials such as Mo_6S_8 [64], Ti_2S_4 [65], TiS_2 [66], CuS [67]. The other particularity of the sulfur cathode is that its electrophilicity makes it incompatible with nucleophilic electrolytes such as Grignard reagent-based electrolytes. In the studies reported so far, the electrolytes used in most magnesium-sulfur batteries are non-nucleophilic [68]. Therefore, the anodic stability and nucleophilicity are two important factors to determine the availability of the electrolyte in magnesium-sulfur batteries.

In general, the oxidation decomposition potential of MACC electrolytes is as high as 3.4 V, which is competent for magnesium-sulfur batteries. As for the compatibility with sulfur, Liu et al soaked the sulfur powder in the 0.04 M MACC/THF ($MgCl_2$:$AlCl_3$ =2:1) electrolyte for 20 days and then tested whether the two reacted [25]. It is found that there is no degradation of the electrolyte according to the change in NMR spectra and color of the MACC solution [25]. Those results indicate that the 0.04 M MACC/THF ($MgCl_2$:$AlCl_3$ =2:1) electrolyte is non-nucleophilic and compatible with sulfur, which is different from the nucleophilic magnesium organohaloaluminate electrolytes.

The reduction of sulfur in 0.06-0.3 M MACC ($MgCl_2$:$AlCl_3$ =2:1) electrolytes with various solvents (THF, DME, DME+DOL, G4+DOL, G4+THF, G4) was also recorded by conducting linear-sweep voltammetry (LSV) test on two-electrode cells with S_8 / SuperP / PVDF as working electrodes and Mg metal as counter/reference electrodes [16a]. The reduction peak current in 0.06 M MACC/THF electrolyte is as low as 12 mA g^{-1}, although control experiments with sulfur-free electrodes demonstrate that this weak reduction peak is indeed a reduction of sulfur. When sulfur loading on the electrode is further reduced by five times, the measured peak current is increased to about 400 mA g^{-1}, indicating that the specific capacity is strongly dependent on the sulfur loading, similar to other metal-sulfur batteries [69]. In addition, the results show that the reduction peaks are different in electrolytes with different solvents, but they are all in the range of 0.49-0.79 V which is lower than the theoretical reduction potential of S_8 for MgS (1.77 V). Similar results are obtained by the discharge curves of Mg-S batteries **(Figure 8b)**. Compared with the performance of MACC electrolytes with different solvents, the smallest polarization in DME+DOL can found, and the sulfur reduction is hard to occur at pristine G4 solvent. In this work, a series of work was done to explore the origin of different reduction potentials. The LSV test of the electrolyte showed that the peak current was significantly increased at high concentration, but the peak position shifted slightly to a lower position. The concentration of active Mg species increased with the increasing electrolyte concentration, as mentioned in the previous chapter, but the polarization of sulfur reduction does not decrease, indicating that the high polarization cannot be attributed to the IR drop and the concentration of the electrochemical active species in this system. In addition, the Mg/Mg symmetric cell with the MACC electrolyte showed low overpotential, suggesting that the polarization is not primarily due to the passivation of Mg. As for the kinetic limitation, the author compared the reduction LSV curves of batteries at 50 ℃ and 21 ℃, and found that the rise of temperature did not increase the reduction potential, indicating that the high overpotential could not be attributed to the kinetic limitation related to S_8 reduction. At last, the author believed that the conditioned electrolyte can react with S due to the presence of free Cl, which may be the reason for the single platform observed in LSV curves.

A MACC-like electrolyte with mononuclear $[Mg\cdot 6THF]^{2+}$ as active species was synthesized by $MgCl_2$ and $AlCl_3$ in ionic liquid n-methyl-(n-butyl) pyrrolidinium bis(trifluoromethanesulfonyl)imide (PYR14TFSI). The Mg-S battery with this electrolyte can deliver a discharge specific capacity of 700 mAh/g and a platform of 0.8 V at 0.01 C. The discharge specific capacity rapidly declined to 130 mAh/g at the fifth cycle [70]. Recently, the research group further explored the application of $MgCl_2$-$AlCl_3$ complexes electrolyte for magnesium sulfur batteries.[71] By adding LiCl to the electrolyte, the battery delivered a discharge specific capacity of about 850 mAh/g and a discharge platform of 1.1 V at 0.1 C.

Up to now, there are few studies on the application of MACC electrolytes in magnesium-sulfur batteries, and the reported performance is nonideal. But after all, magnesium-sulfur chemistry is an emerging electrochemical system, which was first reported in 2010. The MACC electrolyte was discovered even later (in 2014). It is believed that the MACC-based Mg-S batteries with high energy density will be studied extensively in the future because of the high anodic stability, non-nucleophile, free of organic salts, and low-cost characters of electrolytes.

5.3 Application of MACC electrolytes in hybrid batteries

The MACC electrolytes can be matched with the high voltage cathode material due to the high electrochemical window (higher than 3.4 V). The Mg/$LiFePO_4$ hybrid battery can be assembled using $LiFePO_4$ cathode, Mg anode, and a dual-salt electrolyte consisting of 0.2 M $[Mg_2Cl_2 \cdot 4DME][AlCl_4]_2$ and 1.0 M LiTFSI [72]. During the electrochemical reaction, the insertion/extraction of lithium ions occurs at the cathode side, and the deposition/dissolution of Mg occurs at the anode side. The CV curve showed that the overpotential of Mg deposition in the $[Mg_2Cl_2 \cdot 4DME][AlCl_4]_2$/DME electrolyte decreased slightly, and the current density increased slightly after the addition of LiTFSI. The ^{25}Mg NMR spectrum showed that the chemical environment of Mg was unchanged after adding LiTFSI, and it still has a structure in which two Mg^{2+} are bridged by dichloride ligands. The Mg/$LiFePO_4$ battery delivered a high specific capacity of ~ 140 mAh/g at 0.1 C and excellent rate performance **(Figure 8 c and d)** due to the high electrical conductivity and the fast kinetics of Mg deposition/dissolution in the double salt electrolyte.

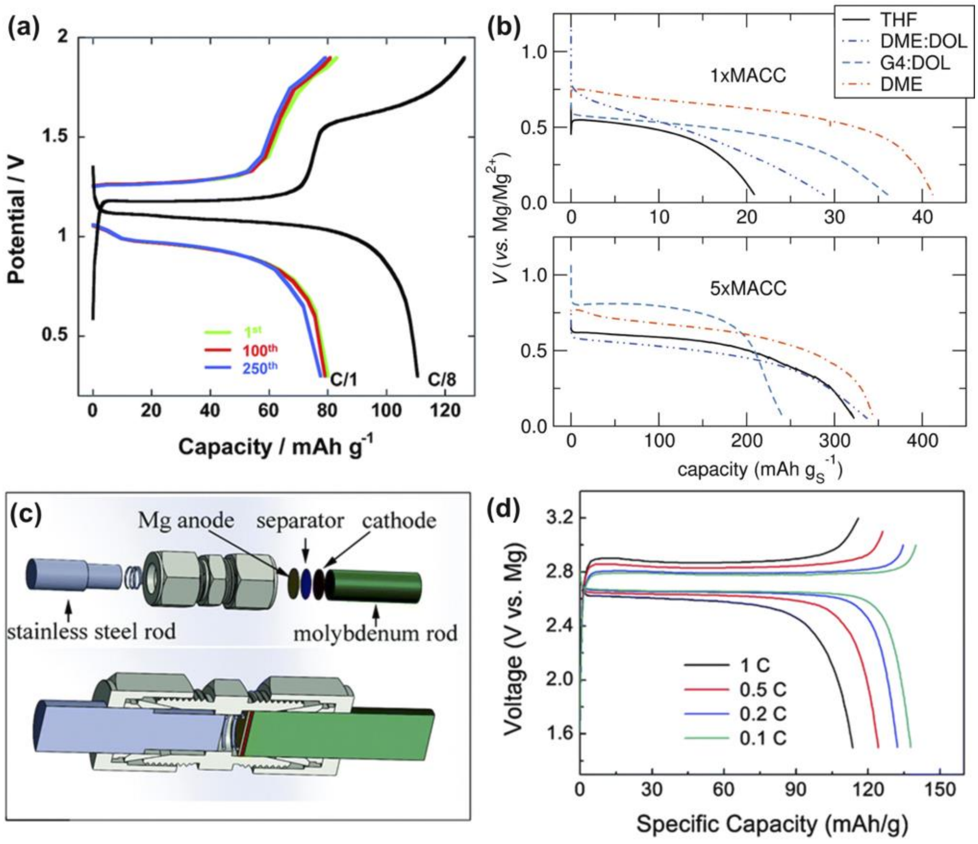

Figure 8. **a** Discharge–charge profiles at the 1st, the 100th, and the 250th cycle of Mg rechargeable batteries with the Chevrel phase cathode at 1C (=128 mA g^{-1}). Reproduced with permission.[49] Copyright 2016, The Royal Society of Chemistry. **b** Galvanostatic discharge profiles of Mg-S batteries with MACC electrolyte at C/50. Reproduced with permission. [16a] Copyright 2019, American Chemical Society. Assembly of prototype hybrid cells and testing results: **c** Schematic illustration of the structure and assembly of the hybrid batteries with Swagelok-type cells, Mo rods, and Mg-Li dual-salt electrolytes consist of 0.2 M $[Mg_2Cl_2(DME)_4][AlCl_4]_2$ and 1.0 M LiTFSI. **d** Typical charge-discharge profiles of the Mg-LEP hybrid batteries at different rates. c, d) Reproduced with permission. [72] Copyright 2013, The Royal Society of Chemistry.

6. Summary and Outlook

In the past few years, a promising inorganic-based MACC electrolyte was developed based on retrosynthesis analysis of $[Mg_2(\mu{-}Cl)_3{\cdot}6THF]^+$, which have been found as the active Mg species in a series of Mg-Cl complex electrolytes. The electrolyte obtained by mixing $MgCl_2$ and $AlCl_3$ in ether contains abundant Cl^- anions. The chloride-containing species in MACC electrolyte is a double-edged sword. It has to be admitted that the corrosion nature of Cl^- does limit the practical application of MACC electrolyte. However, the presence of chloride ions also brings many benefits. For example, the formation of the Mg-Cl complex component helps to improve the deposition and dissolution ability of Mg, and the combination with anions can improve the oxidation stability of electrolytes.

The researches on MACC electrolytes mainly focuses on several aspects. The first is on the synthesis of MACC electrolyte with high deposition/dissolution capability for magnesium. Second, a deep understanding of the Mg species and chemical environment of MACC electrolytes is key to the development of high performance electrolytes. Raman, NMR, XAS, and other in-situ and ex-situ methods are commonly used to study the species in the electrolyte and the electroactive ions enabling Mg deposition and dissolution. DFT calculations are also widely used to explore the chemical environment such as coordination number, ionic structure as well as thermodynamic stability of various Mg species in the electrolyte. The third one is on electrolytic conditioning. For most MACC electrolytes, electrolytic conditioning is a necessary step to achieve high performance electrolytes for reversible electrodeposition of Mg. The electrolyte evolution during the electrolytic conditioning is revealed, which is very important to realize the application of MACC electrolytes in practical Mg batteries. The fresh MACC electrolytes usually contain Mg species such as monomers $[MgCl{\cdot}3THF]^+$, $MgCl_2{\cdot}2THF$, dimers $[Mg_2Cl_3{\cdot}4THF]^+$, $Mg_2Cl_4{\cdot}4THF$ and trimers $[Mg_3Cl_5{\cdot}6THF]^+$, Al species such as $AlCl_4^-$ and $AlCl_2^+$, and impurities such as H_2O and polyTHF. There is an equilibrium among the various Mg species in which the amount of electrochemical active Mg species determines the reversibility of Mg deposition/dissolution in the electrolyte. For fresh MACC electrolyte, the amount of active Mg species can be increased by electrolytic conditioning. At the same time, the Al species that can cause unfavorable co-deposition in the electrochemical cycle is gradually reduced, and free Cl^- anions that can promote the electrodeposition of Mg are generated. Moreover, electrolytic conditioning can remove impurities effectively. The conditioning-free MACC electrolyte was proposed by the introduction of Mg salt or Mg powder to change the equilibrium of Mg species, remove impurities and generate free Cl^-. **(Figure 9)**

Despite the increasing efforts of researchers in this area, the MACC electrolytes still have some shortcomings and unsolved problems. First, the free Cl^- anions in conditioned MACC electrolytes increase the deposition and dissolution kinetics of Mg, but they limit the application of MACC electrolytes in practical batteries due to the inevitable corrosion of Cl^- on battery components. Second, poor temporal stability and the need for re-conditioning to activate are not conducive to the storage and commercialization of the electrolyte. Third, there are few reports on matching with the cathode materials, although it is speculated that it can be applied to magnesium secondary batteries with a variety of cathode material because of its high oxidation decomposition potential. In future research, there are several ways to avoid corrosion caused by chloride ions in the electrolyte. The first is to change the composition of the battery by using a free-standing cathode or a non-metallic collector such as graphite foil. The second is to introduce corrosion inhibitors, which can form a stable passive layer on the metal component. The third is to avoid the formation of free Cl^- and leave the first sheath containing chlorine during the electrochemical reaction. Similar to that in the battery with aqueous electrolyte, where magnesium ions are partial dehydration during intercalation. Fourth, considering the presence of $AlCl_3$ in the electrolyte, DOL solvent may be introduced to synthesize gel or solid electrolyte to reduce the corrosion of chloride ions. To solve the problem of temporal stability, the use of solvents that are not easy to polymerize is an important aspect. Further, attempts can be made to reduce the concentration of Al species in the electrolyte, such as the development of the electrolyte in which both anions and cations are Mg-Cl complexes. This requires us to pay more attention to new synthetic methods, such as magnesium powder as a source of magnesium ions. In addition, from the perspective of the Mg anode, the development of protective film on the Mg anode is also beneficial to improve the chemical stability between the electrolyte and Mg electrode. In order to improve the performance of

MACC electrolytes under practical conditions, the overpotential of Mg deposition and dissolution at different current densities, the uniformity of Mg deposits, and the binding force between the deposited Mg particles and Mg electrode are worthy of further study. It is worth noting that the concentration, solvent, Mg/Al ratio, and raw material purity all affect the composition and performance of MACC electrolytes, so attention should be paid to the adjustment and optimization of these aspects. Meanwhile, the ion immigration, desolvation, and intercalation processes in the Mg batteries with MACC electrolyte need to be studied extensively in the future.

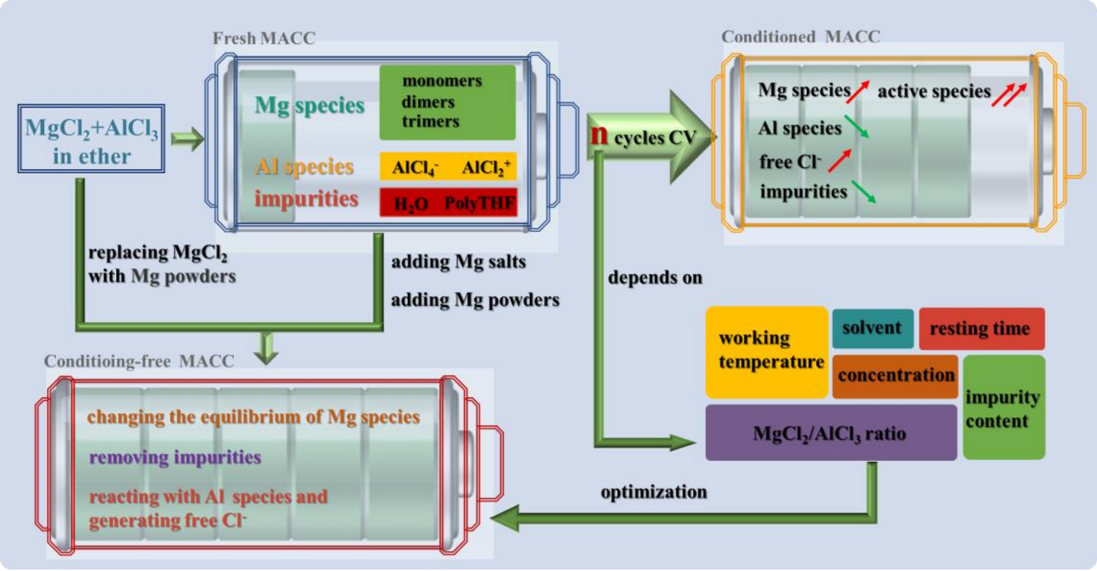

Figure 9. The characteristics of the three MACC electrolytes (fresh, conditioned and conditioning-free) and the relationship between them.

Acknowledgements This research was supported by the National Natural Science Foundation of China (no. 51772068).

Received: ((will be filled in by the editorial staff))
Revised: ((will be filled in by the editorial staff))
Published online: ((will be filled in by the editorial staff))

References

[1] a) J. Muldoon, C. B. Bucur, T. Gregory, *Chemical reviews* **2014**, 114, 11683; b) Y. Zhang,

H. Geng, W. Wei, J. Ma, L. Chen, C. C. Li, *Energy Storage Materials* **2019**, 20, 118; c) J. Bitenc, R. Dominko, *Frontiers in Chemistry* **2018**, 6; d) P. Saha, M. K. Datta, O. I. Velikokhatnyi, A. Manivannan, D. Alman, P. N. Kumta, *Progress in Materials Science* **2014**, 66, 1.

[2] a) M. Jäckle, K. Helmbrecht, M. Smits, D. Stottmeister, A. Groß, *Energy & Environmental Science* **2018**, 11, 3400; b) W. Cao, J. Zhang, H. Li, *Energy Storage Materials* **2020**, 26, 46.

[3] H. D. Yoo, I. Shterenberg, Y. Gofer, G. Gershinsky, N. Pour, D. Aurbach, *Energy & Environmental Science* **2013**, 6, 2265.

[4] D. Aurbach, Z. Lu, A. Schechter, Y. Gofer, H. Gizbar, R. Turgeman, Y. Cohen, M. Moshkovich, E. Levi, *Nature* **2000**, 407, 724.

[5] a) I. Shterenberg, M. Salama, Y. Gofer, E. Levi, D. Aurbach, *MRS Bulletin* **2014**, 39, 453; b) J. Muldoon, C. B. Bucur, A. G. Oliver, T. Sugimoto, M. Matsui, H. S. Kim, G. D. Allred, J. Zajicek, Y. Kotani, *Energy & Environmental Science* **2012**, 5, 5941.

[6] a) T. D. Gregory, R. J. Hoffman, R. C. Winterton, *Journal of the Electrochemical Society* **1990**, 137, 775; b) Z. Lu, A. Schechter, M. Moshkovich, D. Aurbach, *Journal of Electroanalytical Chemistry* **1999**, 466, 203.

[7] a) L. W. F. Gaddum, H. E., *J. Am. Chem. Soc.* **1927**, 49, 1295; b) D. M. M. Overcash, F. C., *Trans. Electrochem. Soc.* **1933**, 64, 305; c) J. H. R. Connor, W. E.; Wood, G. B. , *J. Electrochem. Soc.* **1957**, 104, 38; d) A. Brenner, *J. Electrochem. Soc.* **1971**, 118, 99; e) J. D. Genders, D. Pletcher, *Journal of Electroanalytical Chemistry* **1986**, 199, 93; f) C. Liebenow, *Journal of Applied Electrochemistry* **1997**, 27, 221; g) Z. Z. Feng, Y. Nuli, J. L. Wang, J. Yang, *Journal of the Electrochemical Society* **2006**, 153, C689.

[8] D. Aurbach, G. S. Suresh, E. Levi, A. Mitelman, O. Mizrahi, O. Chusid, M. Brunelli, *Advanced materials* **2007**, 19, 4260.

[9] R. E. Doe, R. Han, J. Hwang, A. J. Gmitter, I. Shterenberg, H. D. Yoo, N. Pour, D. Aurbach, *Chemical communications* **2014**, 50, 243.

[10] R. Deivanayagam, B. J. Ingram, R. Shahbazian-Yassar, *Energy Storage Materials* **2019**, 21, 136.

[11] K. A. See, Y. M. Liu, Y. Ha, C. J. Barile, A. A. Gewirth, *ACS applied materials & interfaces* **2017**, 9, 35729.

[12] a) Y. Gofer, O. Chusid, H. Gizbar, Y. Viestfrid, H. E. Gottlieb, V. Marks, D. Aurbach, *Electrochemical and Solid-State Letters* **2006**, 9, A257; b) N. Pour, Y. Gofer, D. T. Major, D. Aurbach, *Journal of the American Chemical Society* **2011**, 133, 6270; c) Y. Guo, F. Zhang, J. Yang, F. Wang, *Electrochemistry Communications* **2012**, 18, 24.

[13] Y. Viestfrid, M. D. Levi, Y. Gofer, D. Aurbach, *Journal of Electroanalytical Chemistry* **2005**, 576, 183.

[14] P. Canepa, S. Jayaraman, L. Cheng, N. N. Rajput, W. D. Richards, G. S. Gautam, L. A. Curtiss, K. A. Persson, G. Ceder, *Energy Environ. Sci.* **2015**, 8, 3718.

[15] C. J. Barile, R. G. Nuzzo, A. A. Gewirth, *The Journal of Physical Chemistry C* **2015**, 119, 13524.

[16] a) S. C. Bevilacqua, K. H. Pham, K. A. See, *Inorg Chem* **2019**, 58, 10472; b) P. Hegemann, M. Hegemann, L. X. Zan, H. Baltruschat, *Journal of the Electrochemical Society* **2019**, 166, A245.

[17] a) N. N. Rajput, X. Qu, N. Sa, A. K. Burrell, K. A. Persson, *Journal of the American Chemical Society* **2015**, 137, 3411; b) M. Okoshi, Y. Yamada, A. Yamada, H. Nakai, *Journal of the Electrochemical Society* **2013**, 160, A2160.

[18] G. Bieker, M. Salama, M. Kolek, Y. Gofer, P. Bieker, D. Aurbach, M. Winter, *ACS applied materials & interfaces* **2019**, 11, 24057.

[19] H. D. Meerwein, D.; Morschel, H. , *Angew. Chem. Int. Ed.* **1960**, 72.

[20] C. J. Barile, E. C. Barile, K. R. Zavadil, R. G. Nuzzo, A. A. Gewirth, *The Journal of Physical Chemistry C* **2014**, 118, 27623.

[21] S. He, J. Luo, T. L. Liu, *Journal of Materials Chemistry A* **2017**, 5, 12718.

[22] S. He, K. V. Nielson, J. Luo, T. L. Liu, *Energy Storage Materials* **2017**, 8, 184.

[23] K. A. See, K. W. Chapman, L. Zhu, K. M. Wiaderek, O. J. Borkiewicz, C. J. Barile, P. J. Chupas, A. A. Gewirth, *Journal of the American Chemical Society* **2016**, 138, 328.

[24] Y. Cheng, R. M. Stolley, K. S. Han, Y. Shao, B. W. Arey, N. M. Washton, K. T. Mueller, M. L. Helm, V. L. Sprenkle, J. Liu, G. Li, *Physical chemistry chemical physics : PCCP* **2015**, 17, 13307.

[25] T. Liu, Y. Shao, G. Li, M. Gu, J. Hu, S. Xu, Z. Nie, X. Chen, C. Wang, J. Liu, *Journal of Materials Chemistry A* **2014**, 2, 3430.

[26] a) O. Tutusaus, R. Mohtadi, T. S. Arthur, F. Mizuno, E. G. Nelson, Y. V. Sevryugina, *Angewandte Chemie* **2015**, 54, 7900; b) Z. Zhao-Karger, J. E. Mueller, X. Zhao, O. Fuhr, T. Jacob, M. Fichtner, *RSC Advances* **2014**, 4, 26924; c) H. S. Kim, T. S. Arthur, G. D. Allred, J. Zajicek, J. G. Newman, A. E. Rodnyansky, A. G. Oliver, W. C. Boggess, J. Muldoon, *Nature communications* **2011**, 2, 427; d) A. Du, Z. Zhang, H. Qu, Z. Cui, L. Qiao, L. Wang, J. Chai, T. Lu, S. Dong, T. Dong, H. Xu, X. Zhou, G. Cui, *Energy & Environmental Science* **2017**, 10, 2616.

[27] a) H. Xu, Z. Zhang, Z. Cui, A. Du, C. Lu, S. Dong, J. Ma, X. Zhou, G. Cui, *Electrochemistry Communications* **2017**, 83, 72; b) C. Fu, M. B. Oviedo, Y. Zhu, A. von Wald Cresce, K. Xu, G. Li, M. E. Itkis, R. C. Haddon, M. Chi, Y. Han, B. M. Wong, J. Guo, *ACS nano* **2018**, 12, 9775.

[28] T. Liu, J. T. Cox, D. Hu, X. Deng, J. Hu, M. Y. Hu, J. Xiao, Y. Shao, K. Tang, J. Liu, *Chemical communications* **2015**, 51, 2312.

[29] a) Z. Liang, Y. C. Lu, *Journal of the American Chemical Society* **2016**, 138, 7574; b) D.

Szunyogh, R. M. L. McFadden, V. L. Karner, A. Chatzichristos, T. Day Goodacre, M. H. Dehn, L. Formenti, D. Fujimoto, A. Gottberg, E. Kallenberg, I. Kalomista, R. F. Kiefl, F. H. Larsen, J. Lassen, C. D. P. Levy, R. Li, W. A. MacFarlane, I. McKenzie, G. D. Morris, S. Pallada, M. R. Pearson, S. P. A. Sauer, P. Schaffer, P. W. Thulstrup, L. Hemmingsen, M. Stachura, *Dalton transactions* **2018**, 47, 14431; c) W. Zhang, J. Zhu, H. Ang, H. Wang, H. T. Tan, D. Yang, C. Xu, N. Xiao, B. Li, W. Liu, X. Wang, H. H. Hng, Q. Yan, *ACS applied materials & interfaces* **2014**, 6, 7164; d) R. Bhattacharyya, B. Key, H. Chen, A. S. Best, A. F. Hollenkamp, C. P. Grey, *Nature materials* **2010**, 9, 504; e) M. Haouas, F. Taulelle, C. Martineau, *Prog Nucl Magn Reson Spectrosc* **2016**, 94-95, 11.

[30] N. A. Oren Mizrahi, Elad Pollak, Orit Chusid, Vered Marks, Hugo Gottlieb, Liraz Larush, Ella Zinigrad, and Doron Aurbach, *Journal of The Electrochemical Society* **2008**, 155.

[31] Y. Nakayama, Y. Kudo, H. Oki, K. Yamamoto, Y. Kitajima, K. Noda, *Journal of The Electrochemical Society* **2008**, 155, A754.

[32] a) L. F. Wan, D. Prendergast, *Journal of the American Chemical Society* **2014**, 136, 14456; b) P. Canepa, G. S. Gautam, R. Malik, S. Jayaraman, Z. Rong, K. R. Zavadil, K. Persson, G. Ceder, *Chemistry of Materials* **2015**, 27, 3317.

[33] a) S. F. Amalraj, D. Aurbach, *Journal of Solid State Electrochemistry* **2011**, 15, 877; b) A. Benmayza, M. Ramanathan, T. S. Arthur, M. Matsui, F. Mizuno, J. Guo, P.-A. Glans, J. Prakash, *The Journal of Physical Chemistry C* **2013**, 117, 26881.

[34] E. V. Brouillet, A. R. Kennedy, K. Koszinowski, R. McLellan, R. E. Mulvey, S. D. Robertson, *Dalton transactions* **2016**, 45, 5590.

[35] Z. Z. Yeyoung Ha, Christopher J. Barile, Jinho Chang, Ralph G. Nuzzo, Jeffrey Greeley, and Andrew A. Gewirth, *Journal of The Electrochemical Society* **2016**, 163.

[36] J. B. Moss, L. Zhang, K. V. Nielson, Y. Bi, C. Wu, S. Scheiner, T. L. Liu, *Batteries & Supercaps* **2019**, 2, 792.

[37] C. J. Barile, R. Spatney, K. R. Zavadil, A. A. Gewirth, *The Journal of Physical Chemistry C* **2014**, 118, 10694.

[38] Y. He, Q. Li, L. Yang, C. Yang, D. Xu, *Angewandte Chemie* **2019**, 58, 7615.

[39] a) J. G. Connell, B. Genorio, P. P. Lopes, D. Strmcnik, V. R. Stamenkovic, N. M. Markovic, *Chemistry of Materials* **2016**, 28, 8268; b) Y. Vestfried, O. Chusid, Y. Goffer, P. Aped, D. Aurbach, *Organometallics* **2007**, 26, 3130.

[40] J. L. Esbenshade, C. J. Barile, T. T. Fister, K. L. Bassett, P. Fenter, R. G. Nuzzo, A. A. Gewirth, *The Journal of Physical Chemistry C* **2015**, 119, 23366.

[41] J. Qian, W. Xu, P. Bhattacharya, M. Engelhard, W. A. Henderson, Y. Zhang, J.-G. Zhang, *Nano Energy* **2015**, 15, 135.

[42] Z. Song, Z. Zhang, A. Du, S. Dong, G. Li, G. Cui, *Journal of Energy Chemistry* **2020**, 48, 299.

[43] a) J. Muldoon, C. B. Bucur, T. Gregory, *Angew Chem Int Edit* **2017**, 56, 12064; b) S. Yagi, A. Tanaka, Y. Ichikawa, T. Ichitsubo, E. Matsubara, *Research on Chemical Intermediates* **2013**, 40, 3.

[44] J. Luo, S. He, T. L. Liu, *ACS Energy Letters* **2017**, 2, 1197.

[45] I. Shterenberg, M. Salama, H. D. Yoo, Y. Gofer, J.-B. Park, Y.-K. Sun, D. Aurbach, *Journal of The Electrochemical Society* **2015**, 162, A7118.

[46] S. S. Kim, S. C. Bevilacqua, K. A. See, *ACS applied materials & interfaces* **2020**, 12, 5226.

[47] a) Z. Ma, D. R. MacFarlane, M. Kar, *Batteries & Supercaps* **2019**, 2, 115; b) Z. Ma, M. Kar, C. Xiao, M. Forsyth, D. R. MacFarlane, *Electrochemistry Communications* **2017**, 78, 29.

[48] a) S. Hebie, H. P. K. Ngo, J. C. Lepretre, C. Iojoiu, L. Cointeaux, R. Berthelot, F. Alloin, *ACS applied materials & interfaces* **2017**, 9, 28377; b) N. Sa, B. Pan, A. Saha-Shah, A. A. Hubaud, J. T. Vaughey, L. A. Baker, C. Liao, A. K. Burrell, *ACS applied materials & interfaces* **2016**, 8, 16002; c) I.-T. Kim, K. Yamabuki, M. Sumimoto, H. Tsutsumi, M. Morita, N. Yoshimoto, *Journal of Power Sources* **2016**, 323, 51; d) DOI: 10.1002/; e) I.-T. Kim, K. Yamabuki, M. Morita, H. Tsutsumi, N. Yoshimoto, *Journal of Power Sources* **2015**, 278, 340.

[49] J. H. Ha, B. Adams, J.-H. Cho, V. Duffort, J. H. Kim, K. Y. Chung, B. W. Cho, L. F. Nazar, S. H. Oh, *J. Mater. Chem. A* **2016**, 4, 7160.

[50] Y. Li, P. Zuo, N. Zhang, X. Yin, R. Li, M. He, H. Huo, Y. Ma, C. Du, Y. Gao, G. Yin, *Chemical Engineering Journal* **2021**, 403, 126398.

[51] a) M. Du, Q. Li, Y. Zhao, C.-S. Liu, H. Pang, *Coordination Chemistry Reviews* **2020**, 416, 213341; b) Y. Shan, Y. Li, H. Pang, *Advanced Functional Materials* **2020**, 30, 2001298; c) K.-B. Wang, Q. Xun, Q. Zhang, *EnergyChem* **2020**, 2, 100025; d) J. Xu, Z. Wei, S. Zhang, X. Wang, Y. Wang, M. He, K. Huang, *J Colloid Interface Sci* **2020**, 588, 378; e) Q. Xu, H. Pang, H. Xue, Q. Li, S. Zheng, *National Science Review* **2020**, 7, 305.

[52] J. Xu, Z. Wei, W. Yan, P. Chen, J. Li, K. Huang, C. Chen, *Journal of Power Sources* **2021**, 481, 228777.

[53] Y. Li, P. Zuo, R. Li, M. He, Y. Ma, Y. Shi, X. Cheng, C. Du, G. Yin, *Journal of Energy Chemistry* **2019**, 37, 215.

[54] a) S. G. McArthur, R. Jay, L. Geng, J. Guo, V. Lavallo, *Chemical communications* **2017**, 53, 4453; b) T. Mandai, Y. Akita, S. Yagi, M. Egashira, H. Munakata, K. Kanamura, *J. Mater. Chem. A* **2017**, 5, 3152; c) S. Hebie, F. Alloin, C. Iojoiu, R. Berthelot, J. C. Lepretre, *ACS applied materials & interfaces* **2018**, 10, 5527.

[55] L. F. Wan, B. R. Perdue, C. A. Apblett, D. Prendergast, *Chemistry of Materials* **2015**,

27, 5932.

[56] S. Yagi, M. Fukuda, T. Ichitsubo, K. Nitta, M. Mizumaki, E. Matsubara, *Journal of the Electrochemical Society* **2015**, 162, A2356.

[57] a) W. Guo, Y. Fu, *Energy & Environmental Materials* **2018**, 1, 20; b) H.-J. Peng, J.-Q. Huang, X.-B. Cheng, Q. Zhang, *Advanced Energy Materials* **2017**, 7, 1700260.

[58] a) D. Kumar, S. K. Rajouria, S. B. Kuhar, D. K. Kanchan, *Solid State Ionics* **2017**, 312, 8; b) Y.-X. Wang, B. Zhang, W. Lai, Y. Xu, S.-L. Chou, H.-K. Liu, S.-X. Dou, *Advanced Energy Materials* **2017**, 7, 1602829.

[59] a) Q. Zhao, Y. Hu, K. Zhang, J. Chen, *Inorg Chem* **2014**, 53, 9000; b) Y. Liu, Z. Tai, Q. Zhang, H. Wang, W. K. Pang, H. K. Liu, K. Konstantinov, Z. Guo, *Nano Energy* **2017**, 35, 36.

[60] a) J. Zhu, J. Zou, H. Cheng, Y. Gu, Z. Lu, *Green Energy & Environment* **2019**, 4, 345; b) X. Hong, J. Mei, L. Wen, Y. Tong, A. J. Vasileff, L. Wang, J. Liang, Z. Sun, S. X. Dou, *Advanced materials* **2019**, 31, e1802822.

[61] K. A. See, J. A. Gerbec, Y.-S. Jun, F. Wudl, G. D. Stucky, R. Seshadri, *Advanced Energy Materials* **2013**, 3, 1056.

[62] a) P. Wang, M. R. Buchmeiser, *Advanced Functional Materials* **2019**, 29, 1905248; b) M. Rashad, M. Asif, Z. Ali, *Coordination Chemistry Reviews* **2020**, 415, 213312.

[63] a) Z. Zhao-Karger, X. Zhao, D. Wang, T. Diemant, R. J. Behm, M. Fichtner, *Advanced Energy Materials* **2015**, 5, 1401155; b) T. Gao, M. Noked, A. J. Pearse, E. Gillette, X. Fan, Y. Zhu, C. Luo, L. Suo, M. A. Schroeder, K. Xu, S. B. Lee, G. W. Rubloff, C. Wang, *Journal of the American Chemical Society* **2015**, 137, 12388; c) B. P. Vinayan, Z. Zhao-Karger, T. Diemant, V. S. Chakravadhanula, N. I. Schwarzburger, M. A. Cambaz, R. J. Behm, C. Kubel, M. Fichtner, *Nanoscale* **2016**, 8, 3296; d) S. H. Tao Gao, Fei Wang, Zhaohui Ma, Xiaogang Li, Kang Xu, and Chunsheng Wang, *Angew. Chem. Int. Ed.* **2017**,

56, 13526

[64] Y. Cheng, L. R. Parent, Y. Shao, C. Wang, V. L. Sprenkle, G. Li, J. Liu, *Chemistry of Materials* **2014**, 26, 4904.

[65] X. Sun, P. Bonnick, V. Duffort, M. Liu, Z. Rong, K. A. Persson, G. Ceder, L. F. Nazar, *Energy & Environmental Science* **2016**, 9, 2273.

[66] X. Sun, P. Bonnick, L. F. Nazar, *ACS Energy Letters* **2016**, 1, 297.

[67] V. Duffort, X. Sun, L. F. Nazar, *Chemical communications* **2016**, 52, 12458.

[68] a) Z. Zhao-Karger, M. Fichtner, *MRS Communications* **2017**, 7, 770; b) L. Kong, C. Yan, J.-Q. Huang, M.-Q. Zhao, M.-M. Titirici, R. Xiang, Q. Zhang, *Energy & Environmental Materials* **2018**, 1, 100.

[69] a) T. Gao, S. Hou, K. Huynh, F. Wang, N. Eidson, X. Fan, F. Han, C. Luo, M. Mao, X. Li, C. Wang, *ACS applied materials & interfaces* **2018**, 10, 14767; b) H. H. Xu, L. Qie, A. Manthiram, *Nano Energy* **2016**, 26, 224; c) L. Qie, A. Manthiram, *Advanced materials* **2015**, 27, 1694.

[70] W. Li, S. Cheng, J. Wang, Y. Qiu, Z. Zheng, H. Lin, S. Nanda, Q. Ma, Y. Xu, F. Ye, M. Liu, L. Zhou, Y. Zhang, *Angewandte Chemie* **2016**, 55, 6406.

[71] H. Fan, Z. Zheng, L. Zhao, W. Li, J. Wang, M. Dai, Y. Zhao, J. Xiao, G. Wang, X. Ding, H. Xiao, J. Li, Y. Wu, Y. Zhang, *Advanced Functional Materials* **2019**, 30, 1909370.

[72] Y. W. Cheng, D. W. Choi, K. S. Han, K. T. Mueller, J. G. Zhang, V. L. Sprenkle, J. Liu, G. S. Li, *Chemical communications* **2016**, 52, 5379.

Author Photographs

Yaqi Li received his Bachelor's degree in School of Materials Science and Engineering from Harbin Institute of Technology (HIT) in 2014 and 2015. Currently, she is a Ph.D. candidate under supervision of Prof. Pengjian Zuo at HIT. Her research interests are the electrolytes, the interface between Mg electrode and electrolyte and the metal-sulfur batteries.

Pengjian Zuo is currently a Professor in School of Chemistry and Chemical Engineering at Harbin Institute of Technology (HIT). He received the B.E. and Ph.D. degree in Chemical Engineering and Technology at HIT in 2002 and 2007, respectively. He had been a visiting scholar at Pacific Northwest National Laboratory and Brookhaven National Laboratory in 2012–2013 and 2017 respectively. His research interests focus on energy storage materials and high-performance energy storage/conversion systems including lithium/sodium ion batteries, lithium/magnesium sulfur batteries and lithium metal batteries.

Geping Yin is a Professor in School of Chemistry and Chemical Engineering at Harbin Institute of Technology (HIT). She got the B.E. and Ph.D. degree in Electrochemical Engineering at HIT in 1982 and 2000, respectively. She has been to Yokohama National University as a visiting scholar in 2008. She continuously entered the list of the Elsevier Most Cited Chinese Researchers in 2015 and 2016. Her research focuses on advanced electrochemical catalysis, advanced electrode materials for LIBs and other chemical power sources systems.